The development of BCC_RAD radiative transfer model and its applications

Hua Zhang

（huazhang@cma.gov.cn)

State Key Laboratory of Severe Weather,

Chinese Academy of Meteorological Sciences, Beijing, China


张华 编著
BCC_RAD DAQI FUSHE CHUANSHU MOS
BCC_RAD大气辐射
传输模式
气象出版社
China Meteorological Press

Chapters

1. Correlated k-Distribution Method for Atmospheric Absorption
2. Aerosol Optics
3. Cloud Optics
4. Radiative Transfer Algorithms
5. Comparison between BCC_RAD and Different Radiation Models
6. Applications in RF and GWP studies
7. Applications in BCC_AGCM

Outline

1. **Correlated k-Distribution Method**
2. Aerosol Optics
3. Cloud Optics
4. Radiative Transfer Algorithms
5. Comparison of BCC_RAD with other Models

Methods for Overlapping
(Zhang et al., JGR, 2003)

- Completely Uncorrelated
- Perfectly Correlated
- Partly Correlated

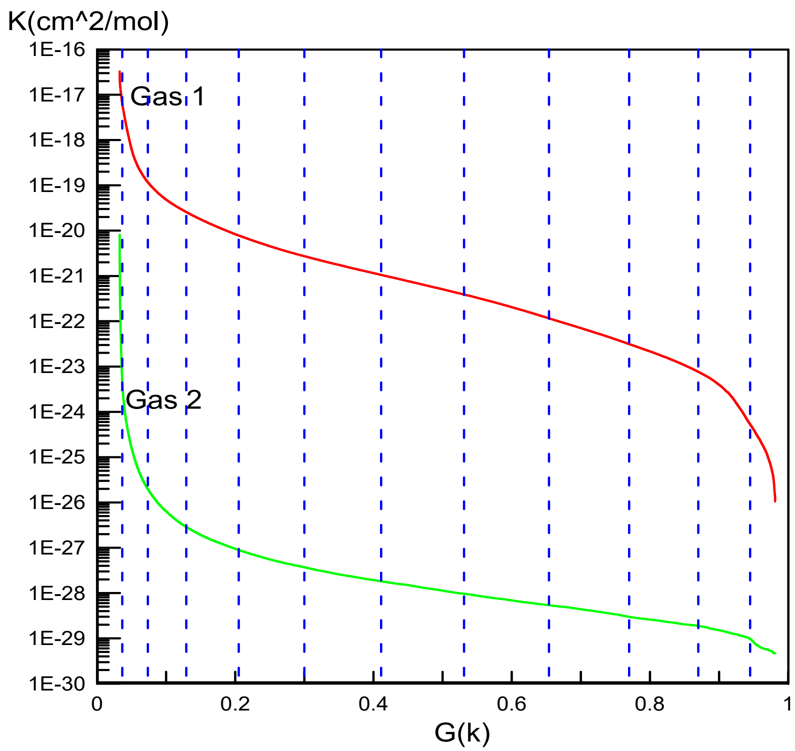

Scheme I: Completely uncorrelated:

Formula-1 $$T(u_1,u_2)=T(u_1)T(u_2) = \sum_{\substack{i=1,M \\ j=1,N}} A_i A_j \exp\left[-\left(k_i^1 u_1 + k_j^2 u_2\right)\right]$$

Scheme II: Perfectly correlated:

Formula-2 $$T(u_1,u_2)=\sum_{j=1}^{N} A_j \exp\left[-\left(k_j^1 u_1 + k_j^2 u_2\right)\right]$$

Problems of Above Two Schemes

- Scheme-I:

*Underestimates or overestimates transmittance (Shi, 1984; Chou et al., 2001);

*Cannot be used in some remote sensing applications (Yang et al., 2000);

- Scheme-II:

*Overestimates transmittance for most cases (Firsov et al., 1998).

Correlation among Gases

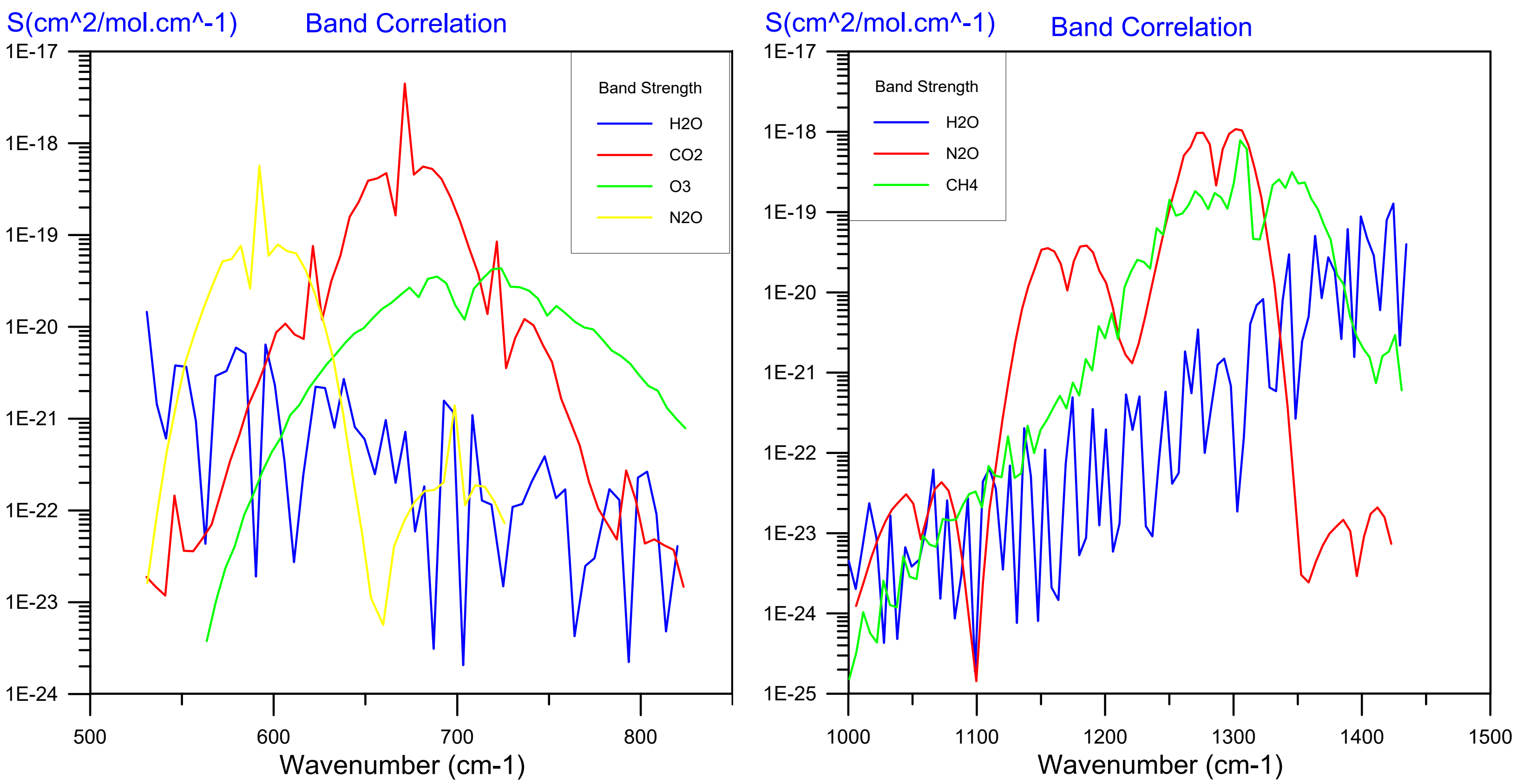

Scheme III: partly correlated

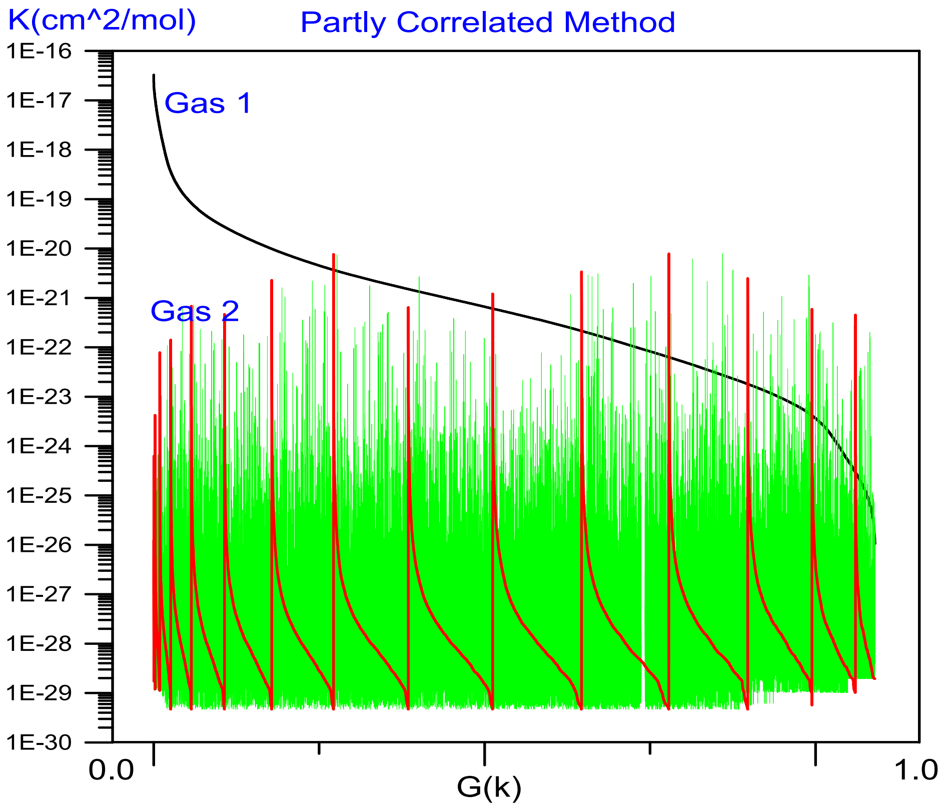

Formula-4

$$T(u_1, u_2) = \sum_{i=1}^{M} A_i \exp\left[-\left(k_i^1 u_1 + k_i^2 u_2\right)\right]$$

Formula-5

$$T(u_1, u_2) = \sum_{i=1}^{M} A_i \exp\left[-\left(k_i^1 u_1 + \overline{k_i^2} u_2\right)\right]$$

Flow Chart for Calculation

(Zhang et al., JGR, 2003)

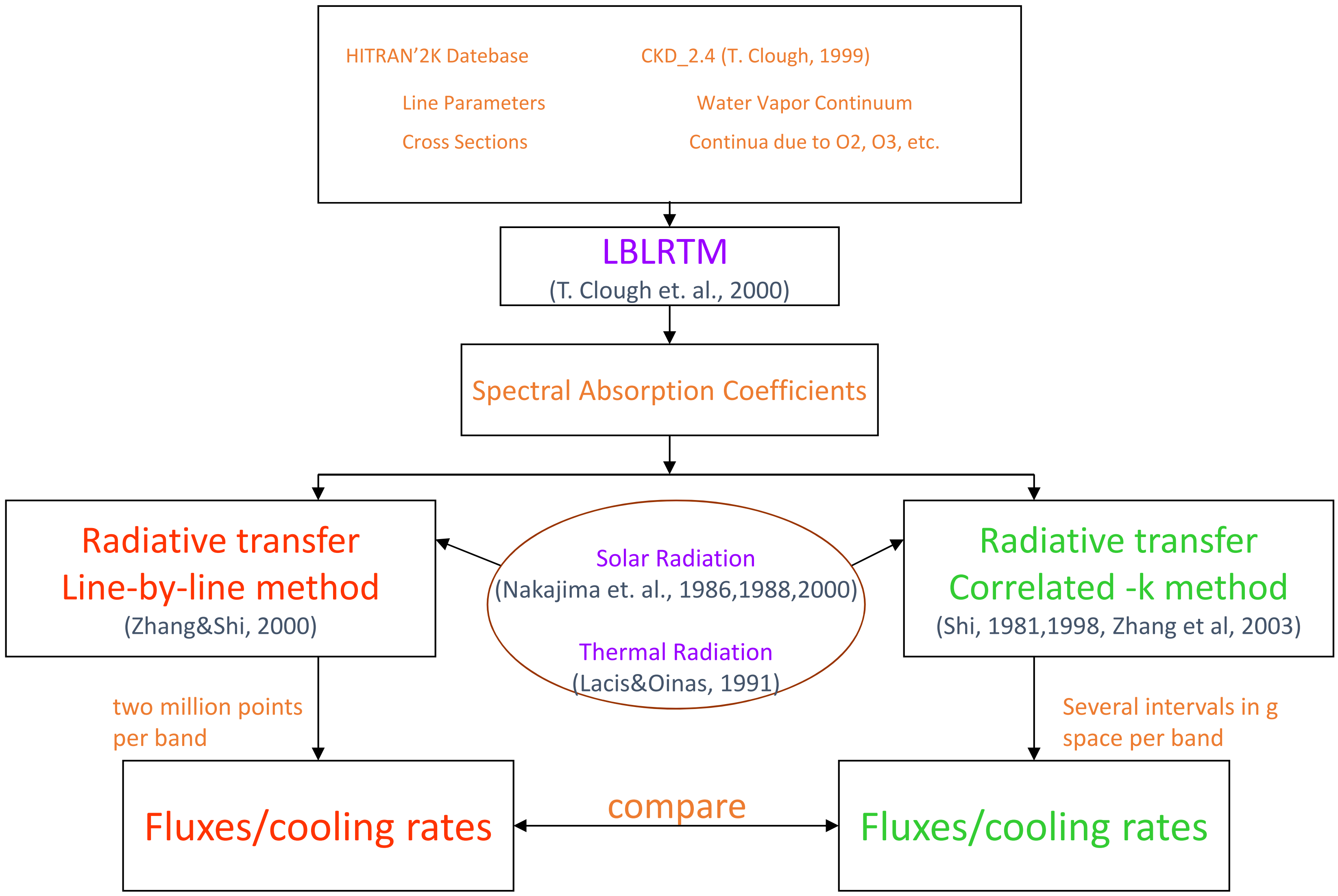

Optimal method to chose overlapping bands （Zhang et al., JQSRT, 2006a)

- Criteria

$$Diff = \frac{1}{Mlayer \cdot Natm} \sum_{\substack{layer=1 \\ iatm=1}}^{\substack{Natm \\ Mlayer}} (CR_{\substack{layer \\ iatm}}^{ck-D} - CR_{\substack{layer \\ iatm}}^{LBL})^2$$

$$Method = Method[Min(Diff1, Diff2, Diff3, Diff4),...]$$

Mlayer=75; Natm=6;

1. Tropical;
2. Mid-Lat summer;
3. Mid-Lat winter;
4. High-Lat summer;
5. High-Lat winter;
6. US standard.

Band Configuration

Band	Wavenumber (cm^{-1})	*k*-interval	Gases	Transmittance model
1	10 - 250	12	H_2O	
2	250 - 430	14	H_2O	
3	430 - 530	16	H_2O	
4	530 - 630	14	H_2O, CO_2, N_2O	Formula-1
5	630 - 700	16	H_2O, CO_2, O_3	Formula-5
6	700 - 820	16	H_2O, CO_2, O_3	Formula-1
7	820 - 940	6	H_2O	
8	940 - 1200	10	H_2O, CO_2, O_3	Formula-1
9	1200 - 1300	9	H_2O, CH_4	Formula-4
10	1300 - 1390	14	H_2O, N_2O, CH_4	Formula-1
11	1390 - 1480	16	H_2O	
12	1480 - 1810	14	H_2O	
13	1810 - 2110	10	H_2O	
14	2110 - 2680	14	H_2O, CO_2, N_2O	Formula-1
15	2680 - 3500	8	H_2O, CH_4	Formula-2
16	3500 - 3900	15	H_2O, CO_2	Formula-2
17	3900 - 4540	16	H_2O, CH_4	Formula-5
18	4540 - 6150	16	H_2O	
19	6150 - 8050	15	H_2O	
20	8050 -12000	16	H_2O	
21	12000-22000	3	H_2O, O_3	Formula-5
22	22000-31000		---	
23	31000-33000	2	O_3	
24	33000-35000	2	O_3	
25	35000-37000	2	O_3	
26	37000-43000	4	O_3, O_2	Formula-1
27	43000-49000	2	O_3, O_2	Formula-5

Sensitivity to Concentration

2 × CO2 (330 ppmv) Results

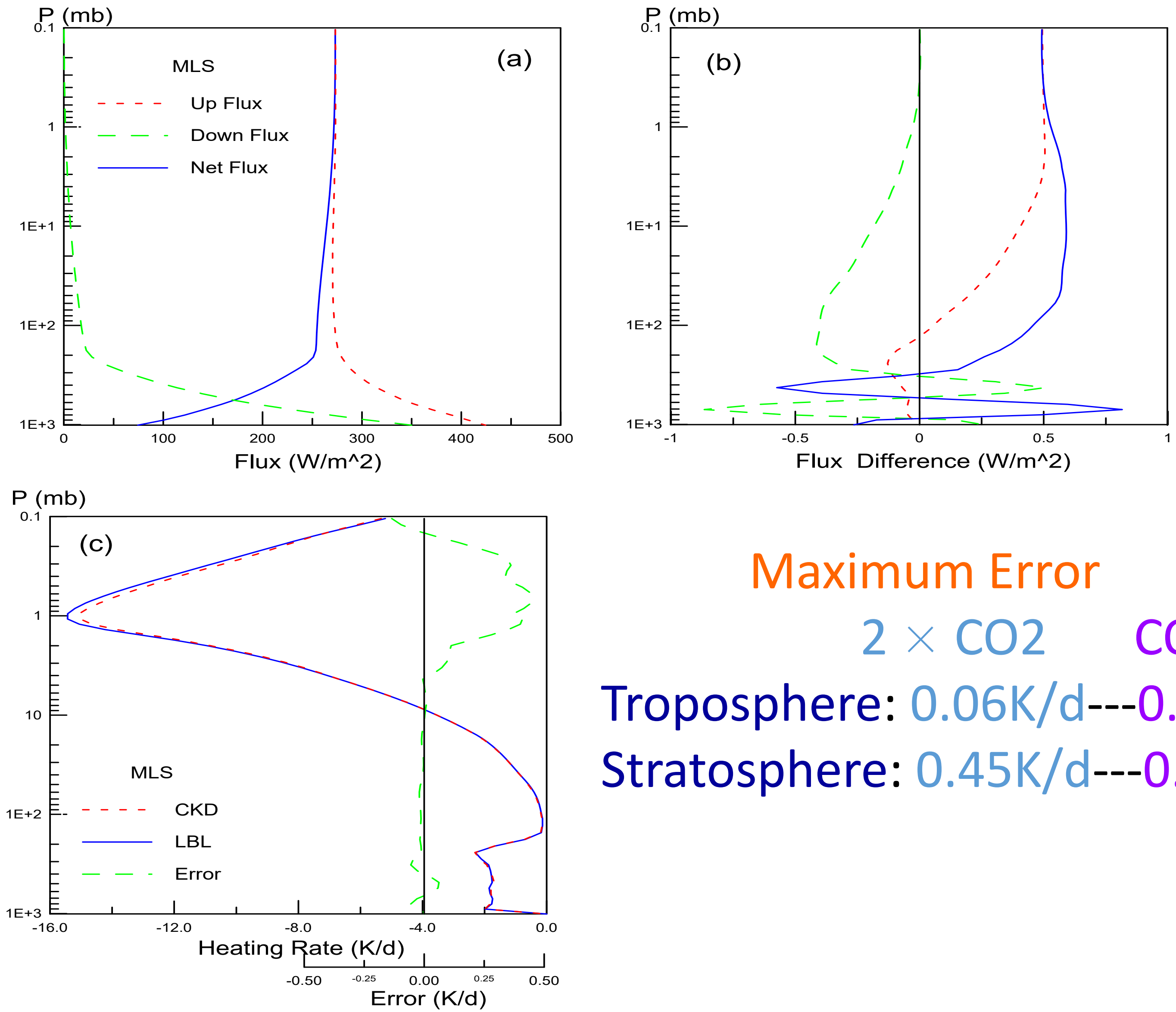

Maximum Error

2 × CO2 CO2

Troposphere: 0.06K/d---0.06K/d;

Stratosphere: 0.45K/d---0.33K/d;

Maximum Errors of LW Heating Rates For 42 Diverse Profiles (Garand et al., 2001)

Troposphere

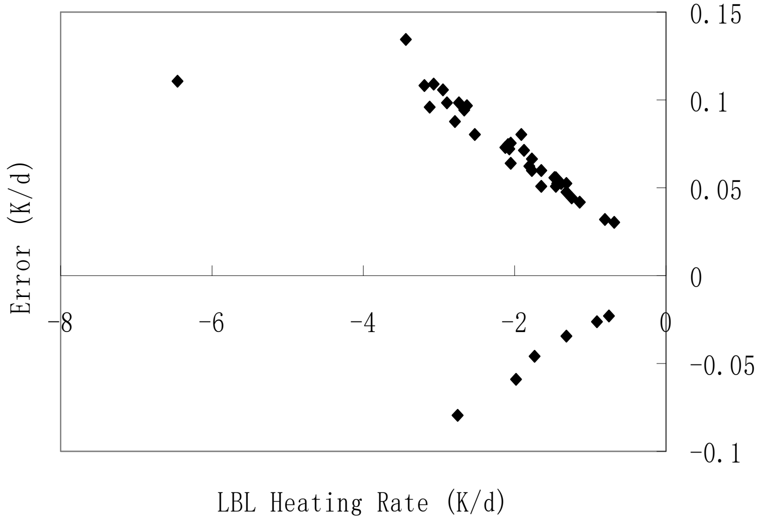

Stratosphere

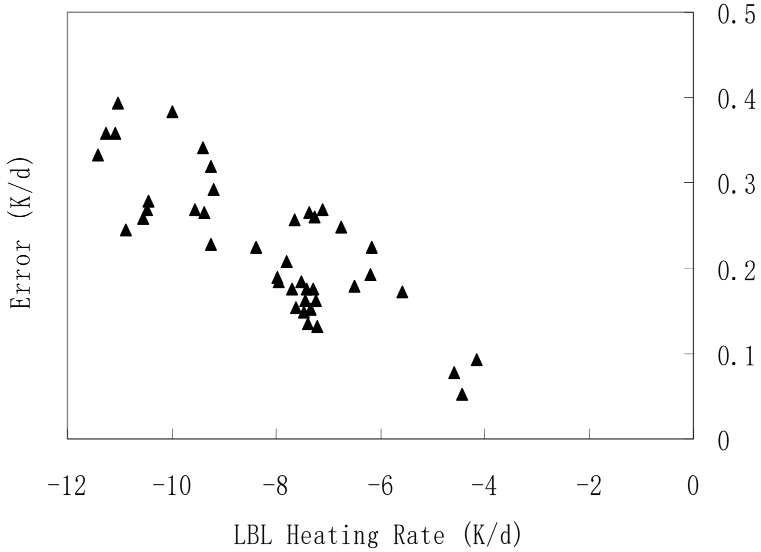

Average Value

Troposphere: 0.068K/d;

Stratosphere: 0.22K/d;

Maximum Errors of LW Net Fluxs For 42 Diverse Profiles

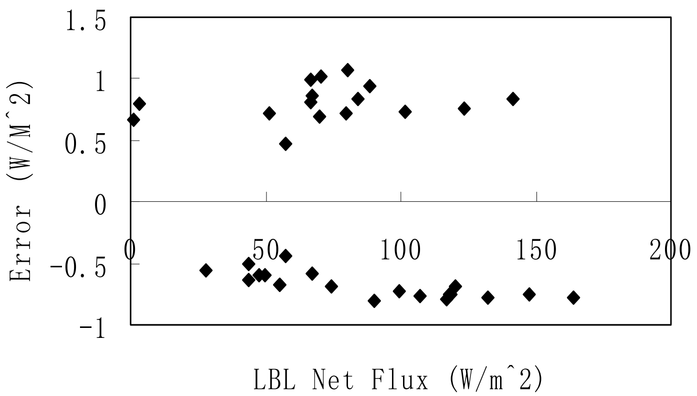

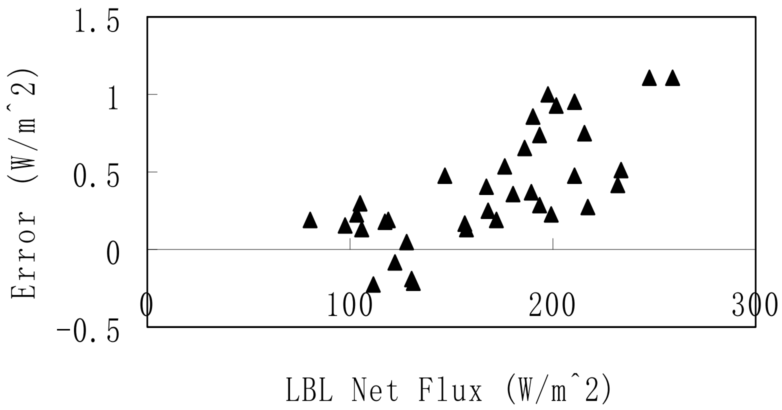

Acuracy of Net Flux:
1.1 W/m2

Five versions in 17-band scheme

Band	Region (cm^{-1})	Gas	5 Versions				
			17H	17M	17L1	17L2	17L3
1	10–250	H_2O	12	12	4	4	4
2	250–550	H_2O	16	15	15	4	4
3	550–780	H_2O, CO_2	16	16	16	16	11
4	780–990	H_2O	5	5	5	5	5
5	990–1200	H_2O, O_3	9	9	5	5	5
6	1200–1430	H_2O, N_2O, CH_4	14	12	5	5	5
7	1430–2110	H_2O	8	5	5	5	5
8	2110–2680	H_2O, CO_2, N_2O	15	14	2	2	2
9	2680–5200	H_2O	16	6	5	5	5
10	5200–12,000	H_2O	7	7	5	5	5
11	12,000–22,000	H_2O, O_3	3	3	3	3	3
12	22,000–31,000	—	0	0	0	0	0
13	31,000–33,000	O_3	2	2	2	2	2
14	33,000–35,000	O_3	2	2	2	2	2
15	35,000–37,000	O_3	2	2	2	2	2
16	37,000–43,000	O_3, O_2	4	4	4	4	4
17	43,000–49,000	O_3, O_2	2	2	2	2	2
Total number of k-intervals			133	116	82	71	66

The selection of number of k-interval (Zhang et al., Optical Engineering, 2006b)

Band Configurations for different users

N	17-band (cm^{-1})	Gas	21-band (cm^{-1})	Gas	27-band (cm^{-1})	Gas	55-band (cm^{-1})	Gas
1	10	H_2O	10	H_2O	10	H_2O	10	H_2O
2	250	H_2O	250	H_2O	250	H_2O	50	H_2O
3	550	H_2O,CO_2	430	H_2O	430	H_2O	60	H_2O
4	780	H_2O	530	H_2O, CO_2, N_2O	530	H_2O, CO_2, N_2O	80	H_2O
5	990	H_2O, O_3	630	H_2O, CO_2, O_3	630	H_2O,CO_2, O_3	100	H_2O
6	1,200	H_2O, N_2O, CH_4	700	H_2O, CO_2, O_3	700	H_2O, CO_2, O_3	120	H_2O
7	1,430	H_2O	820	H_2O	820	H_2O	160	H_2O
8	2,110	H_2O,CO_2, N_2O	940	H_2O, CO_2, O_3	940	H_2O, CO_2, O_3	220	H2O
9	2,680	H_2O	1,200	H_2O, N_2O, CH_4	1,200	H_2O, CH_4	280	H_2O
10	5,200	H_2O	1,430	H_2O	1,300	H_2O, N_2O, CH_4	350	H_2O
11	12,000	H_2O, O_3	2,110	H_2O, CO_2, N_2O	1,390	H_2O	430	H_2O
12	22,000	—	2,680	H_2O, CO_2, CH_4	1,480	H_2O	530	H_2O, CO_2, N_2O
13	31,000	O_3	4,540	H_2O, CO_2	1,810	H_2O	630	H_2O, CO_2, O_3
14	33,000	O_3	6,150	H_2O	2,110	H_2O, CO_2, N_2O	700	H_2O, CO_2, O_3
15	35,000	O_3	12,000	H_2O, O_3	2,680	H_2O, CH_4	820	H_2O
16	37,000	O_3, O_2	22,000	—	3,500	H_2O, CO_2	940	H_2O, CO_2, O_3
17	43,000	O_3, O_2	31,000	O_3	3,900	H_2O, CH_4	1,110	H_2O, CO_2, O_3
18	49,000		33,000	O_3	4,540	H_2O	1,200	H_2O, N_2O, CH_4
19			35,000	O_3	6,150	H_2O	1,350	H_2O, CH_4
20			37,000	O_3, O_2	8,050	H_2O	1,430	H_2O
21			43,000	O_3, O_2	12,000	H_2O, O_3	1,600	H_2O
22			49,000		22,000	—	1,810	H_2O, CO_2, O_3
23					31,000	O_3	2,110	H_2O, CO_2, N_2O
24					33,000	O_3	2,380	CO_2, N_2O
25					35,000	O_3	2,680	H_2O, CH_4
26					37,000	O_3, O_2	3,080	H_2O, N_2O
27					43,000	O_3, O_2	3,400	H_2O, CO_2
28					49,000		3,890	H_2O, CH_4
29							4,540	H_2O, CO_2
30							5,400	H_2O
31							6,150	H_2O, CO_2
32							7600	H_2O, O_2
33							8050	H_2O
34							10,000	H_2O
35							12,000	O_3, O_2
36							13,200	H_2O, O_3
37							14,500	H_2O, O_3
38							16,000	H_2O, O_3
39							18,000	H_2O, O_3
40							20,000	O_3
41							22,000	—
42							29,000	O_3
43							31,000	O_3
44							33,000	O_3
45							35,000	O_3
46							37,000	O_3, O_2
47							39,000	O_3, O_2
48							41,000	O_3, O_2
49							43,000	O_3, O_2
50							45,000	O_3, O_2
51							47,000	O_3, O_2
52							49,000	O_3, O_2
53							51,000	O_3, O_2
54							53,000	O_3, O_2
55							55,000	O_2
							57,000	

Outline

1. Correlated k-Distribution Method
2. Aerosol Optics
3. Cloud Optics
4. Radiative Transfer Algorithms
5. Comparison of BCC_RAD with other Models

Spherical Aerosols

(Zhang et al., 2012; 王志立，博士论文，2011）

Mie Theory:
Sulfate, OC, BC, Nitrate, Sea Salt

Real part of the refractive index of nitrate

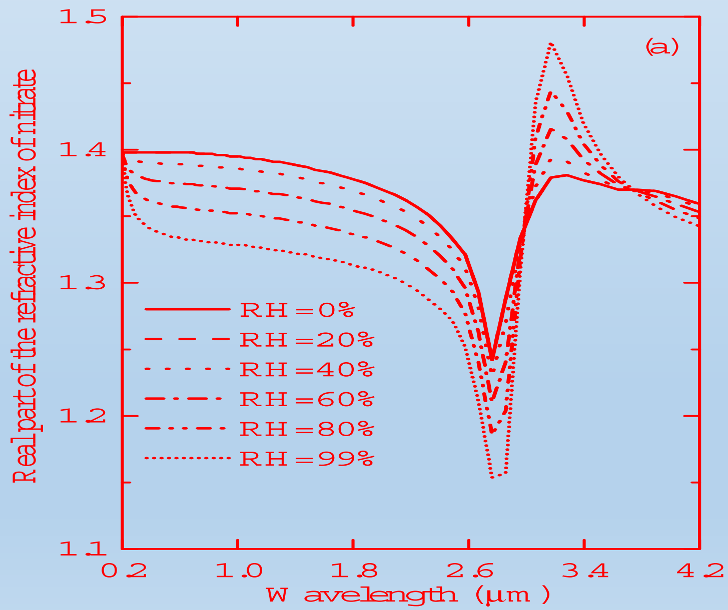

Ratio of real part (Nitrate/Sulfate)

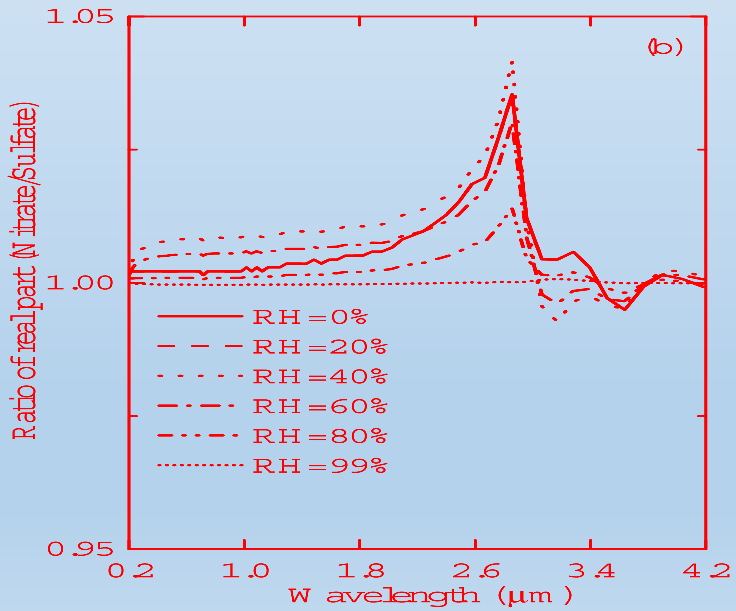

Nonspherical dust-like aerosols

(卫晓东和张华，光学学报，2011；卫晓东，硕士论文，2010)

The shape of dust particle is irregular. The rotational symmetry ellipsoid is used to approximate the shape of the actual dust particle.

The distribution of dust particles is described by lognormal distribution:

$$n(r_v) = \frac{dN(r_v)}{dr_v} = \frac{1}{r_v}\frac{N}{\sqrt{2\pi}\ln\sigma}\exp\left[-\frac{1}{2}\left(\frac{\ln r_v - \ln r_m}{\ln\sigma}\right)^2\right]$$

OPAC (Optical Properties of Aerosols and Clouds) model divides dust aerosols into four types:

Aerosol types	Mode radius, r_m(μm)	Standard Deviation, б	Density, ρ(g/cm^3)	mass concentration(μg m^{-3})/(part cm^{-3})
Nuclei mode (MINM)	0.07	1.95	2.60	2.78E-2
Accumulation mode (MIAM)	0.39	2.00	2.60	5.53E0
Coarse mode (MICM)	1.90	2.15	2.60	3.24E2
Transmission mode (MITR)	0.50	2.20	2.60	1.59E1

Nonspherical dust-like aerosols

Change of Qe (a), ω (b) and g (c) of four types of dust-like aerosols with wavelength

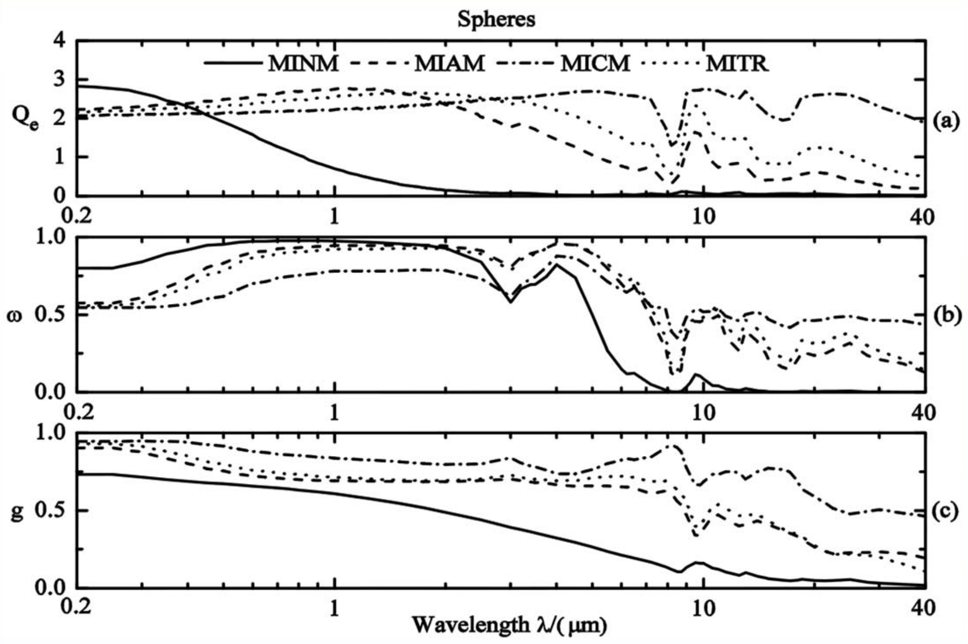

Change of ratios of Qe(a),ω(b)and g(c) of spheroid to those of sphere with wavelength

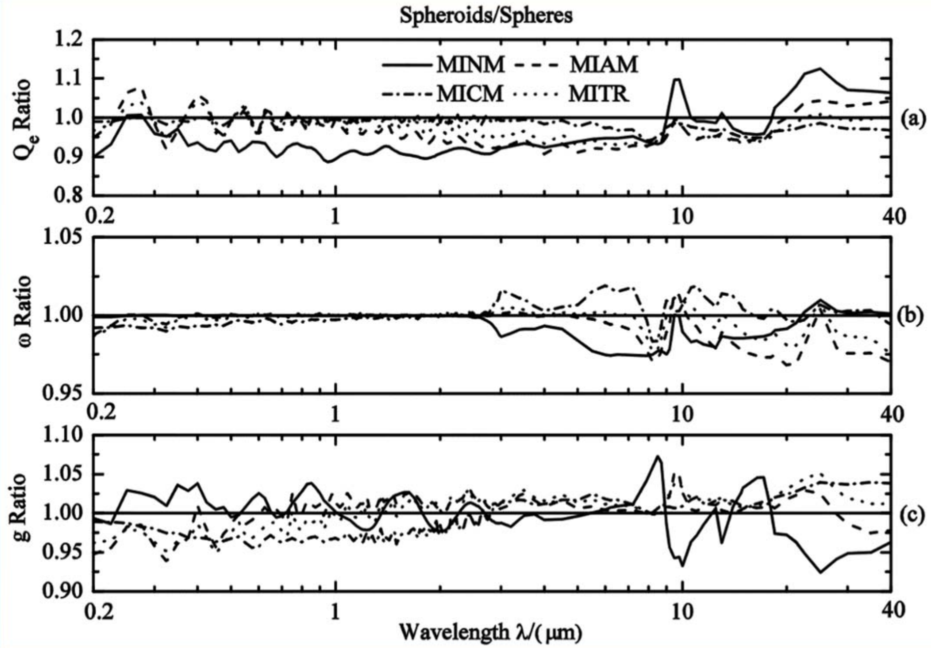

The shape of dust-like aerosols has a smaller influence on the extinction efficiency factor, scattering albedo and asymmetry factor compared to the size distribution

Summary

第 31 卷 第 5 期 光 学 学 报 Vol. 31, No. 5
2011 年 5 月 ACTA OPTICA SINICA May, 2011

非球形沙尘气溶胶光学特性的分析

卫晓东[1,2] 张 华[2]

([1] 中国气象科学研究院，北京 100081
[2] 国家气候中心中国气象局气候研究开放实验室，北京 100081)

摘要 将 T 矩阵方法与几何光学方法相结合，精确计算了从太阳短波到红外谱段具有一定形状分布和谱分布的非球形沙尘粒子的光学特性，并与等体积球形沙尘的光学特性进行了比较。结果表明：1）相比沙尘粒径大小分布对沙尘气溶胶消光效率因子，单次散射反照率以及不对称因子的影响，沙尘形状对上述参数的影响明显偏小；2）非球形与球形沙尘粒子的相函数在短波区存在显著差异，这种差异在卫星探测常用的可见光区达到最大，并且随着散射角的变化具有一定的规律；3）在短波区，雷达方程中的消光后向散射比受沙尘形状的影响比较显著，因此在利用雷达方程反演沙尘气溶胶光学厚度时应考虑非球形效应。

关键词 大气光学；光学特性；T 矩阵方法；几何光学方法；沙尘气溶胶；非球形粒子

the retrieval of dust optical depth by lidar.

Different mixing of aerosols

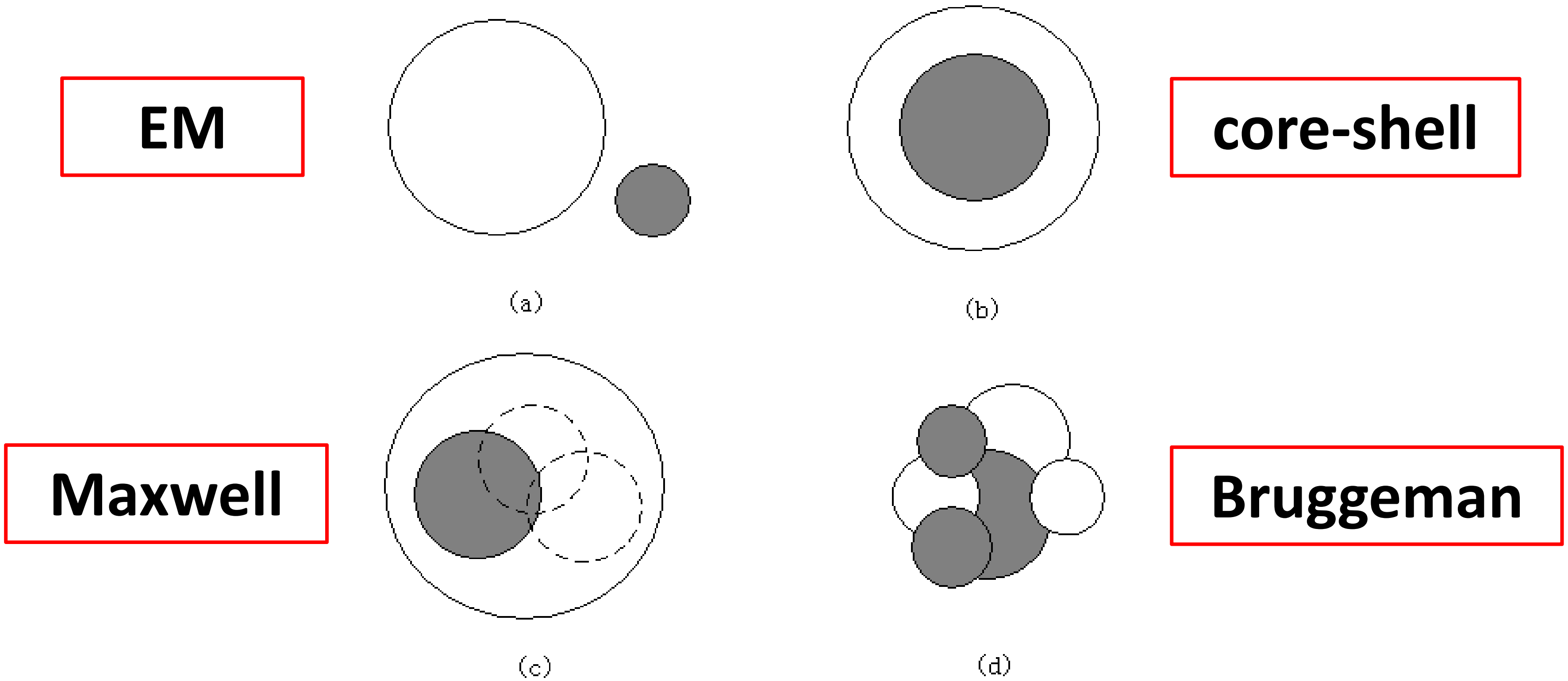

Mixing models considered in BCC_RAD

The optical properties of aerosols

- Complex refractive indices are from HITRAN 2005 database.
- The optical properties of BC-sulfate and BC-OC aerosols including17 Wave bands: 0.204– 1000 μm, 6 relative humidity bins: 0.2 – 0.99, 10 volume mixing ratio bands: 10%~9

复折射指

EM optics

xwell optics

ggeman optics

re-shell optics

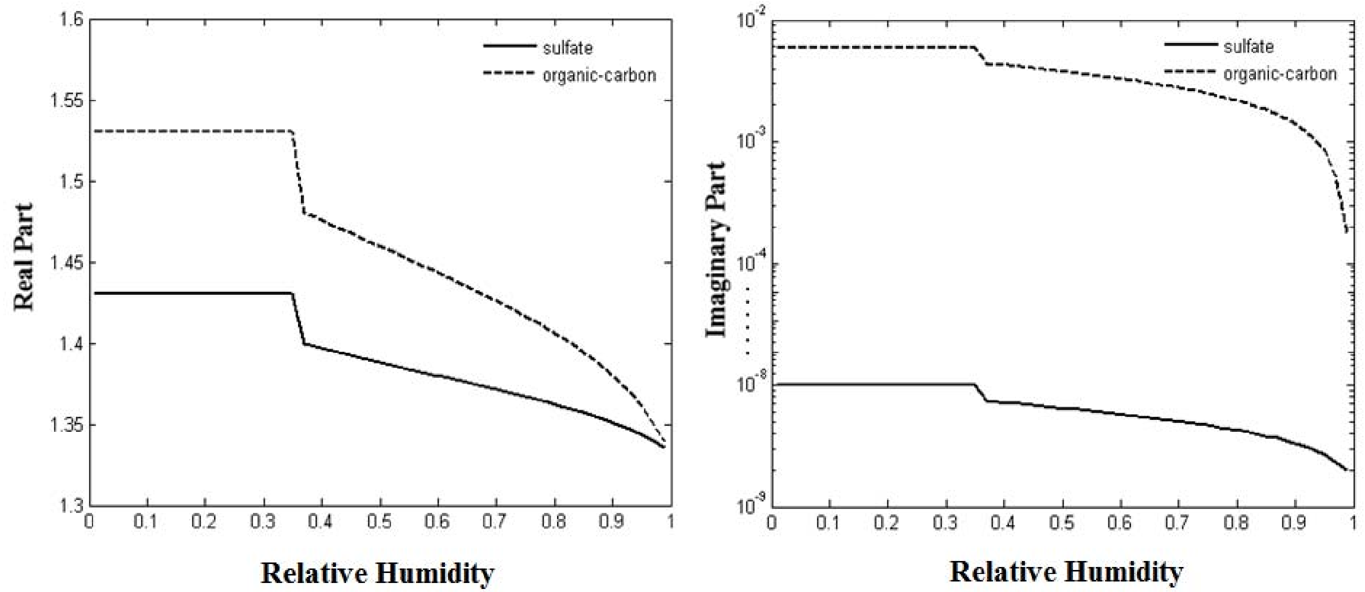

The change of refractive indices with radii growth（Borhen *et al.*, 1998）

Maxwell equivalent media（Garnett *et al.*, 1904）

$$m = \sqrt{m_a^2 \frac{m_b^2 + 2m_a^2 + 2f_b(m_b^2 - m_a^2)}{m_b^2 + 2m_a^2 - f_b(m_b^2 - m_a^2)}}$$

$$m = m_w + (m_d - m_w) \times \frac{(r_d)^3}{(r_m)^3}$$

Bruggeman equivalent media（Niklasson *et al.*, 1981）

$$f_a \frac{m_a^2 - m^2}{m_a^2 + 2m^2} + f_b \frac{m_b^2 - m^2}{m_b^2 + 2m^2} = 0$$

The optical properties of aerosols
(Zhang et al., JQSRT, 2015a)

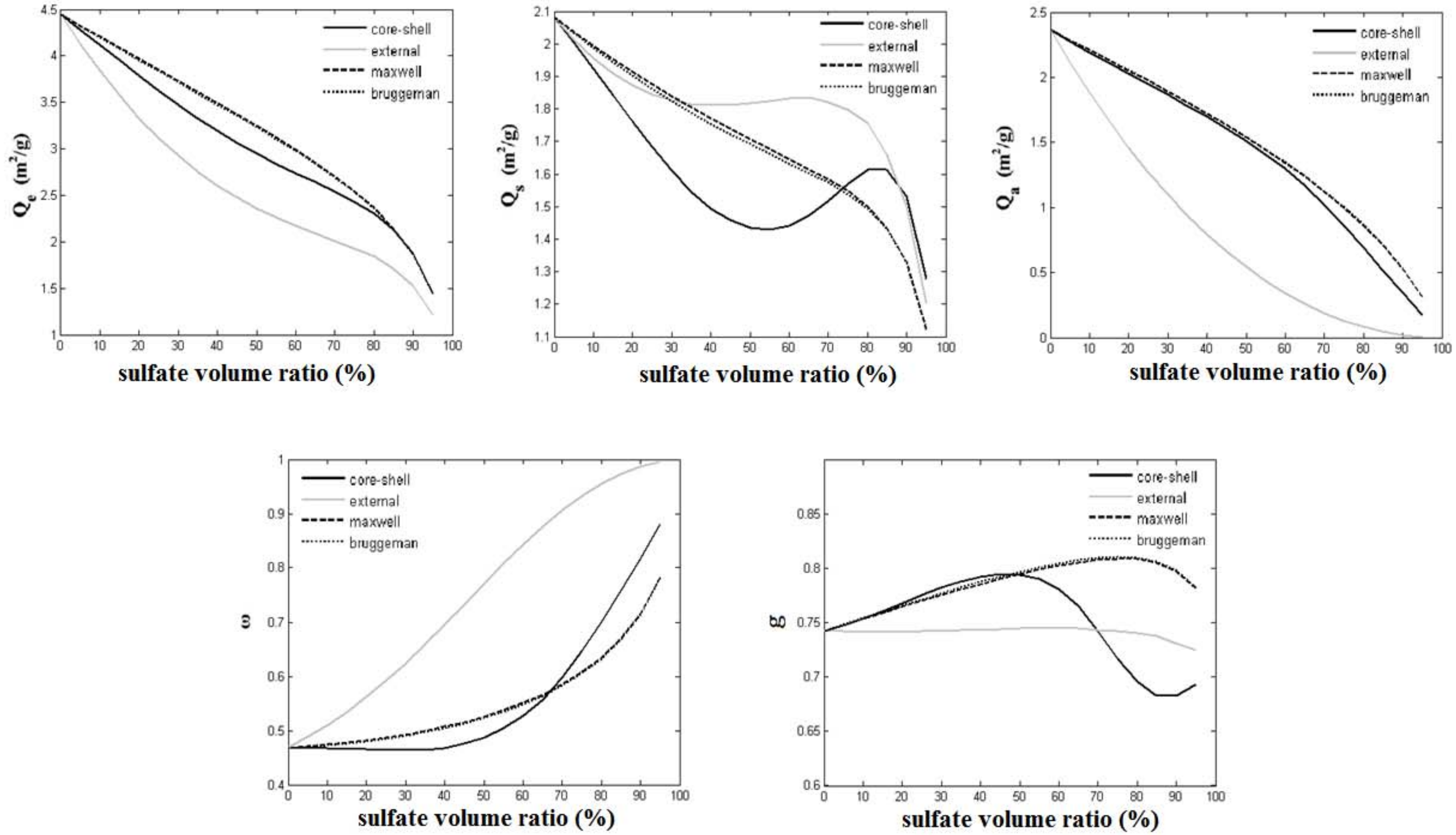

The change of BC-sulfate aerosol optical properties with sulfate volume ratio

The optical properties of aerosols

(Zhang et al., JQSRT, 2015a)

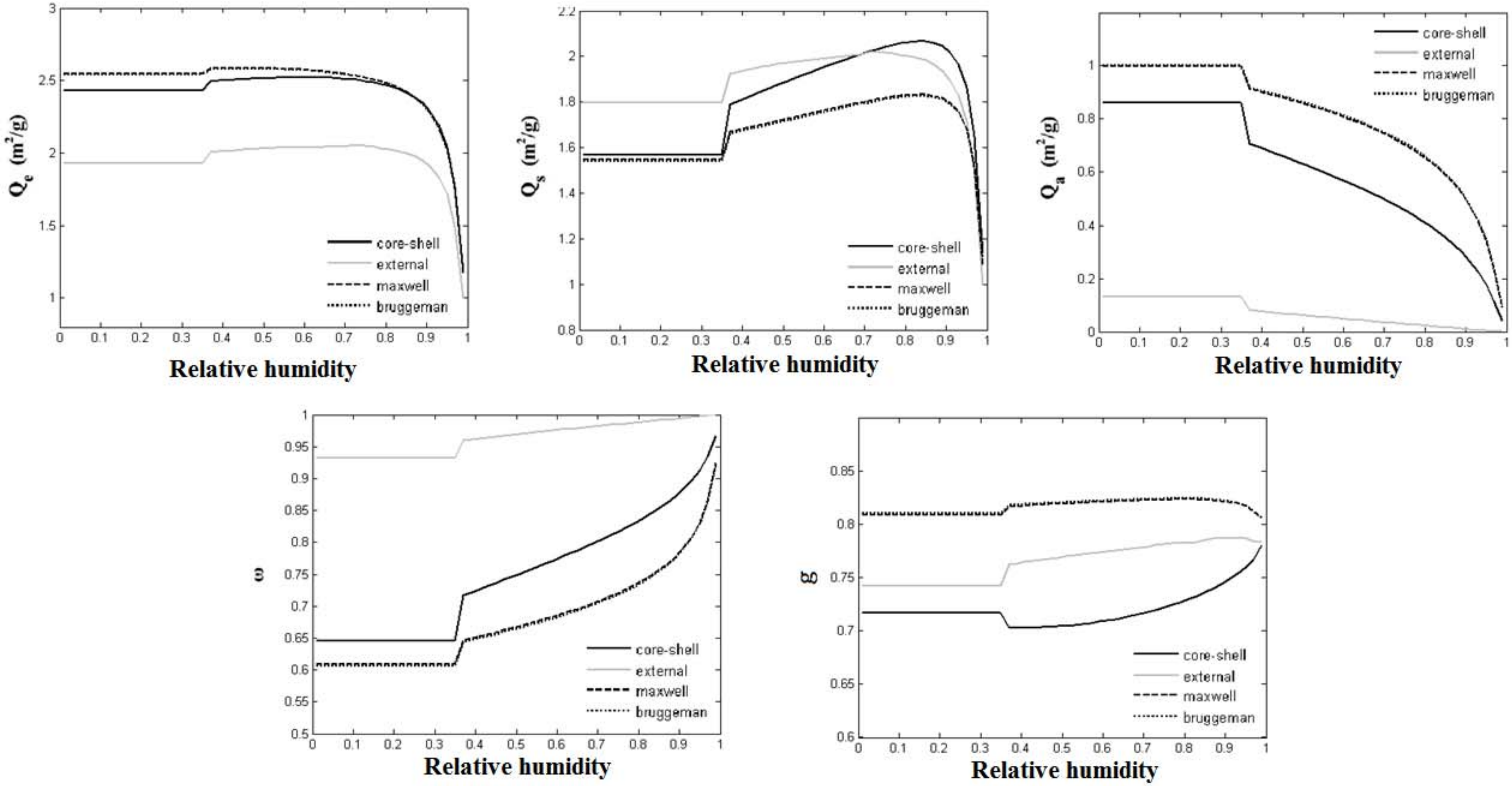

The change of BC-sulfate aerosol optical properties with relative humidity

Outline

1. Correlated k-Distribution Method
2. Aerosol Optics
3. Cloud Optics
4. Radiative Transfer Algorithms
5. Comparison of BCC_RAD with other Models

1、Optical Properties of Water Cloud

Water cloud optical properties

(卢鹏，博士论文，2012；Lu et al., JAS, 2011)

Band-mean parameterization

- ignores the correlation between gaseous absorption and cloud optical properties in the band
- overestimates the heating rate at the top of cloud in shortwave

k- distribution parameterization

- considers the correlation
- improves the precision of radiation calculation of cloudy sky

The correlation of the optical properties between water cloud and water vapor

Rearranging Kabs of water vapor.

Mapping the optical properties of water clouds.

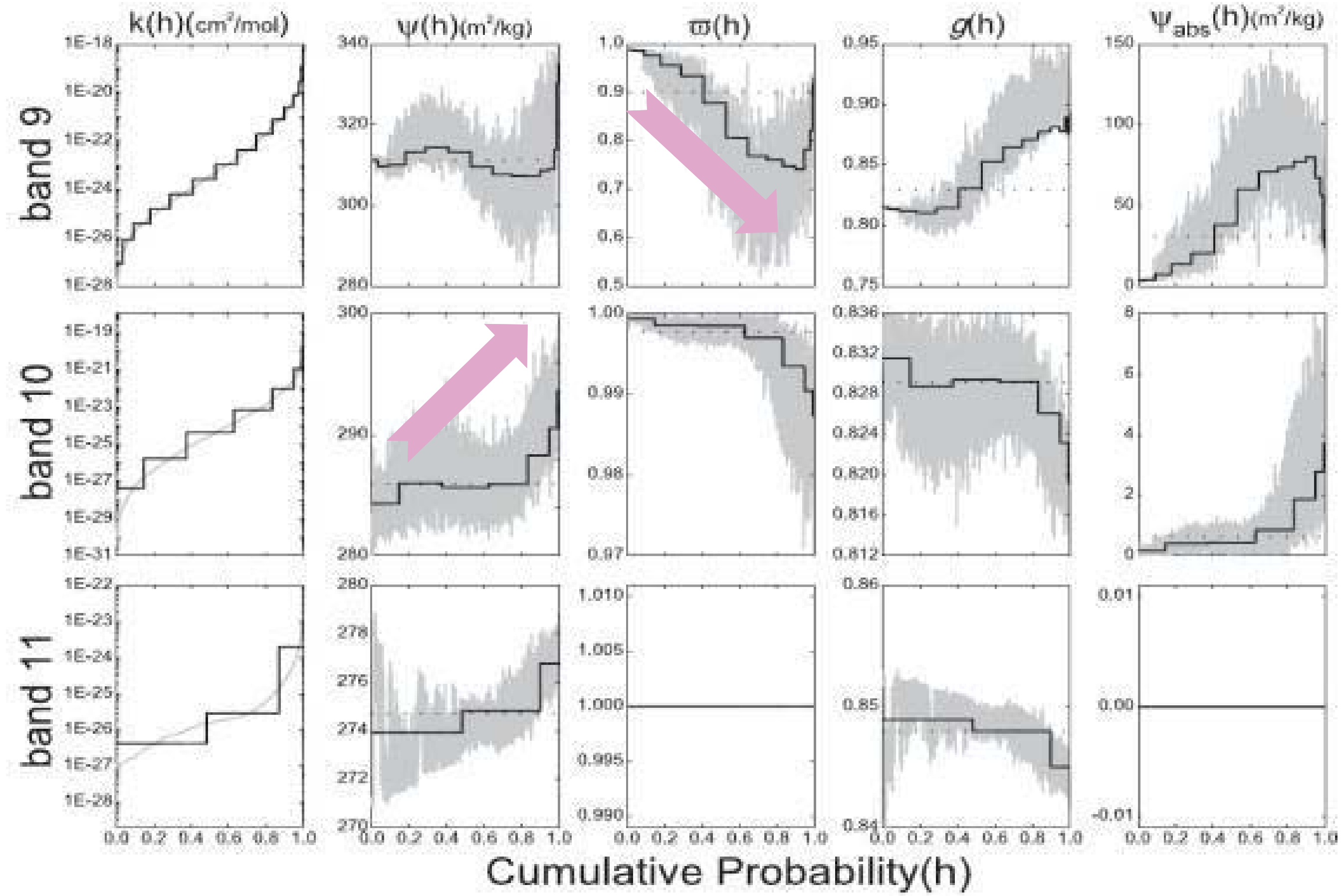

(Lu et al, JAS, 2011)

The effect of two schemes of water cloud on radiative flux and heating rate

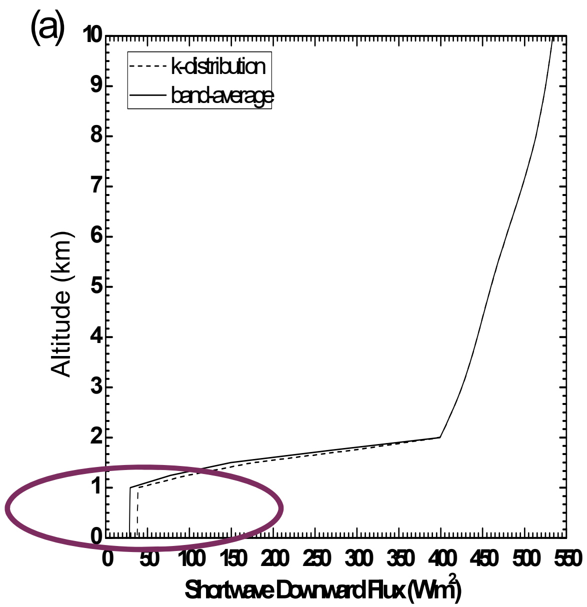

短波向下辐射通量

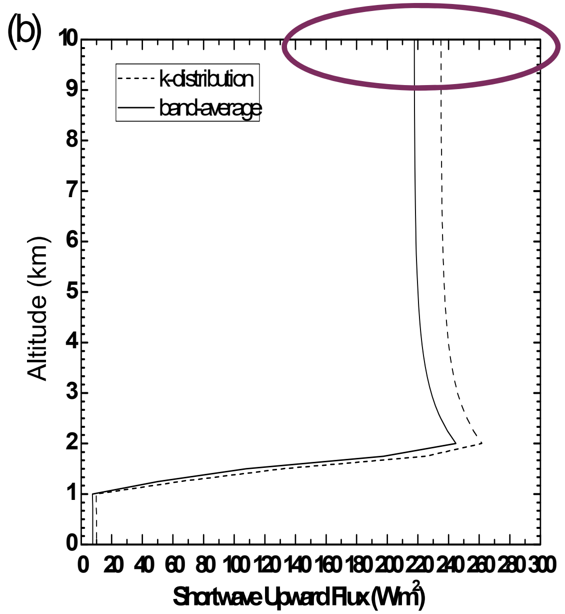

短波向上辐射通量

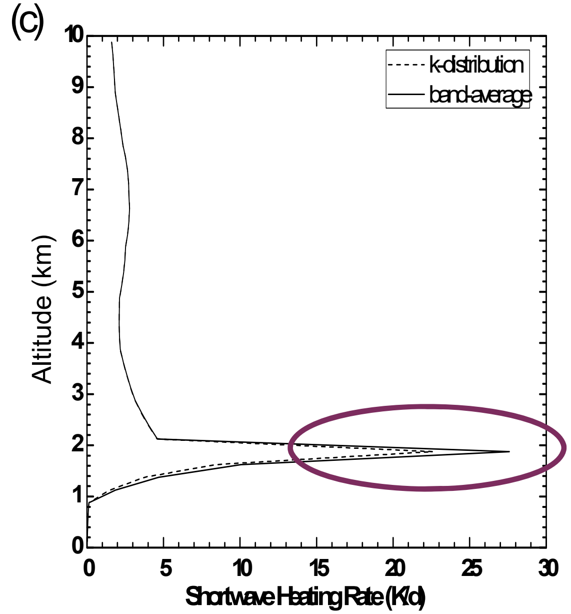

短波加热率

Optical Properties of Water Cloud

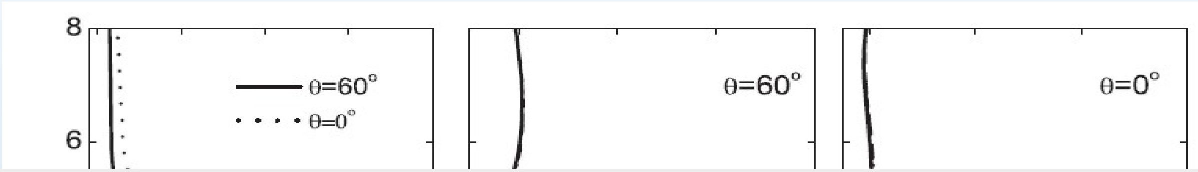

Compared to the band-mean scheme, the k-distribution cloud scheme can reduce the overestimation of shortwave heating rate at the top of cloud.

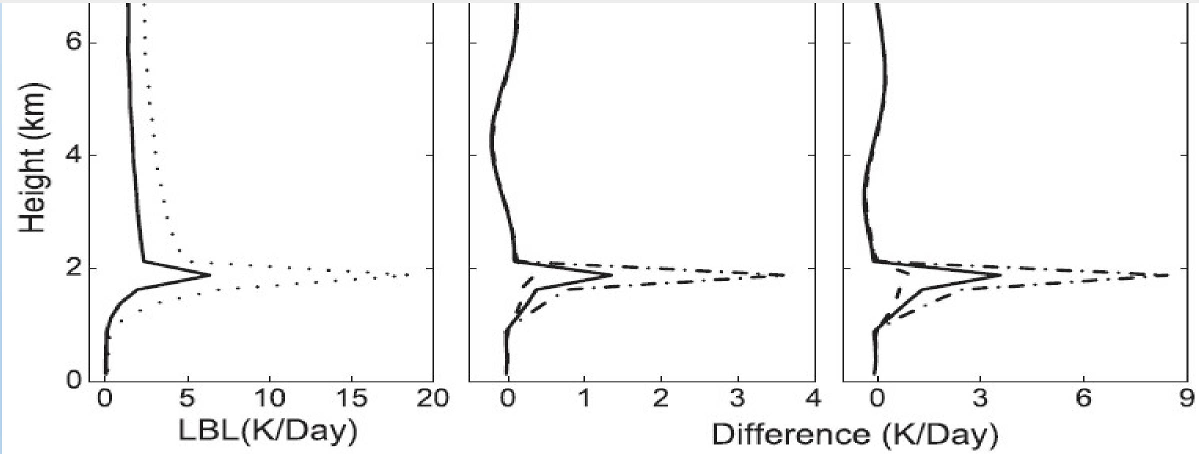

Left: Shortwave heating rate by LBL for the middle and low clouds, in MLS profile with solar zenith angle $\theta_0=0^o$ and $\theta_0=60^o$.
Middle: The errors for $\theta_0=60^o$.
Right: The errors for $\theta_0=0^o$

(Lu et al., JAS, 2011)

2、New parameterization for ice cloud

(Zhang et al, JQSRT, 2015b)

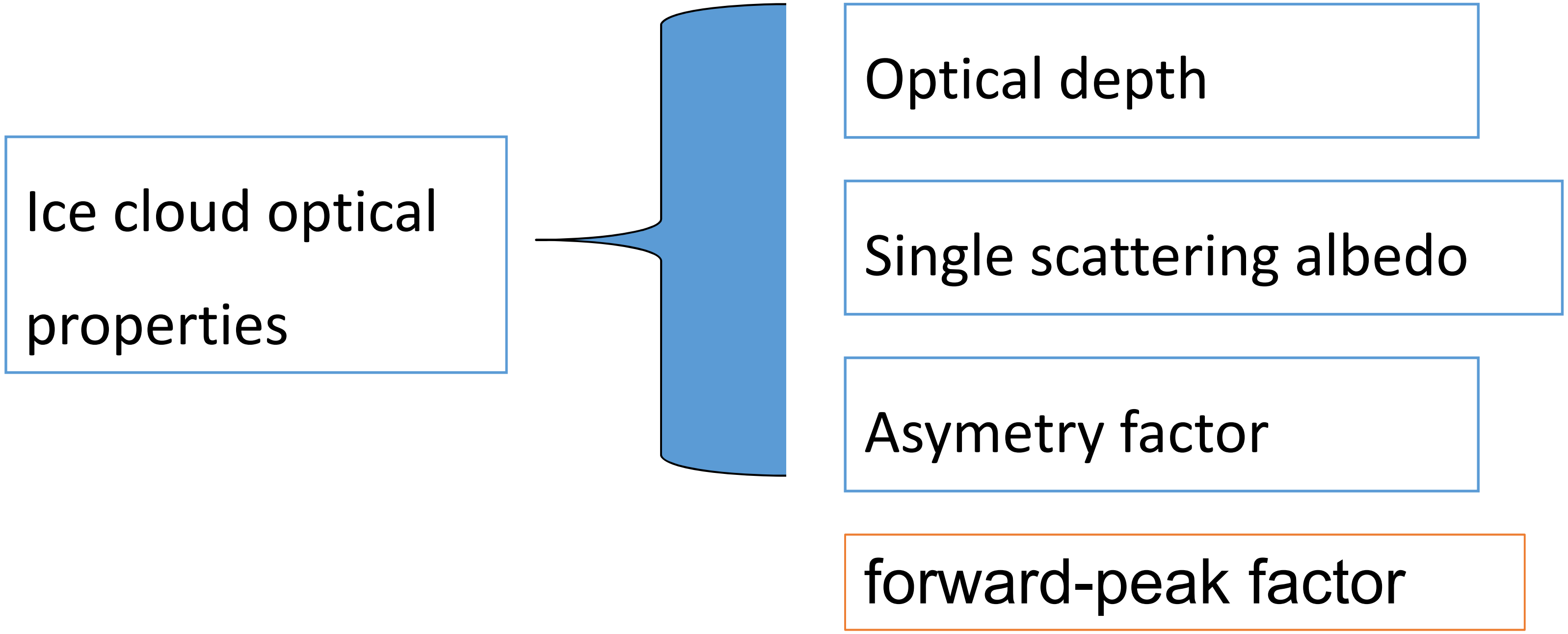

Habits in the dataset

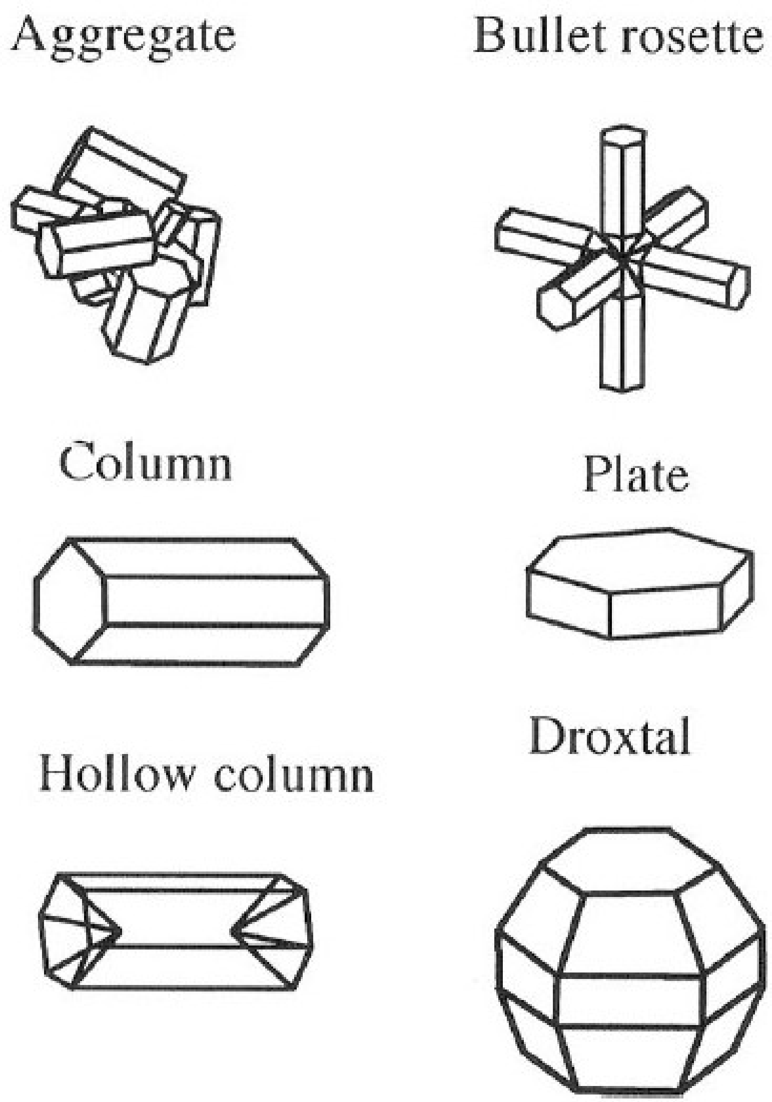

Method

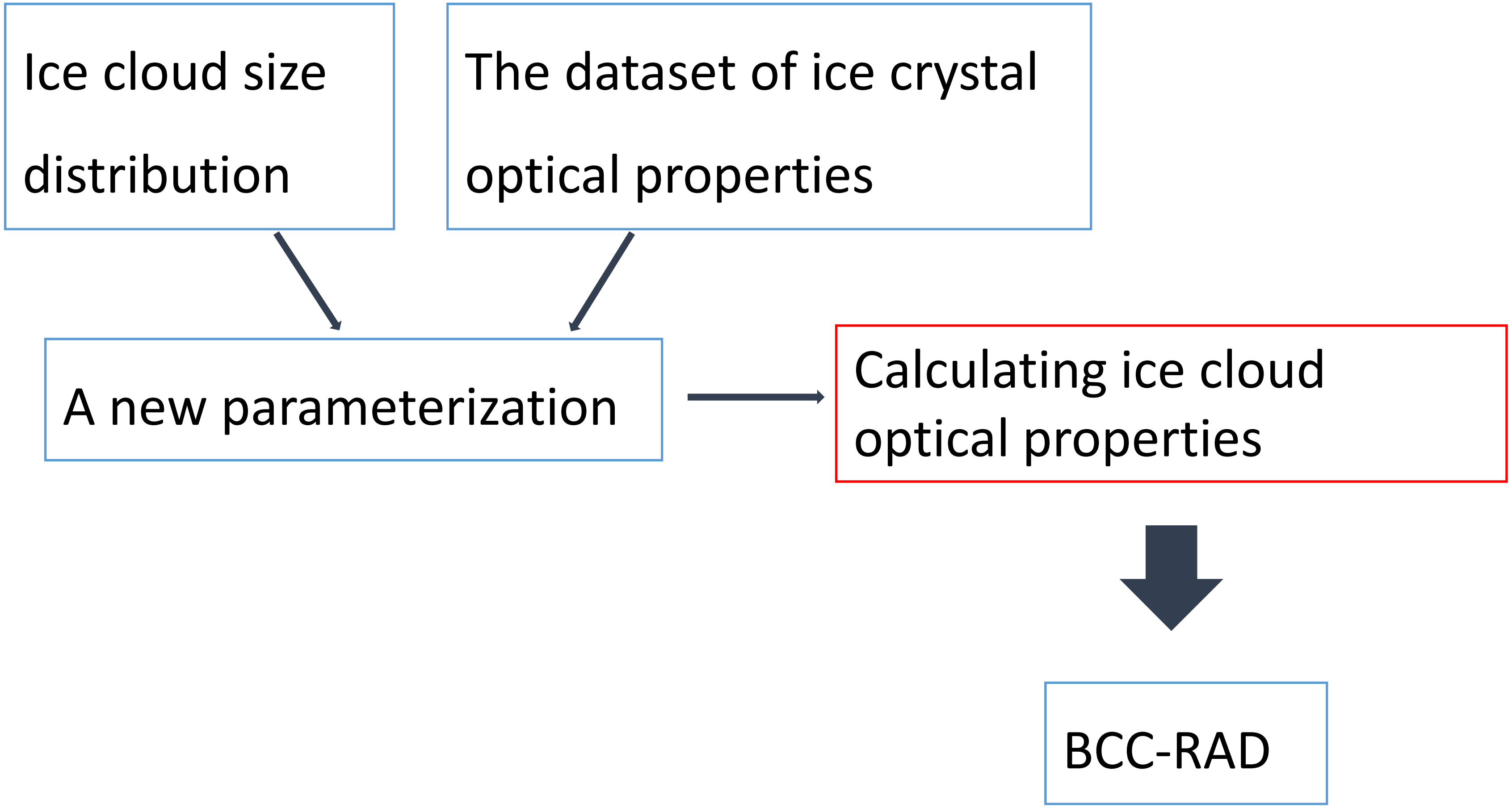
Ice cloud size distribution
The dataset of ice crystal optical properties
A new parameterization
Calculating ice cloud optical properties
BCC-RAD

Data

- Ice crystal particles: six habits.
- Geometric properties: equivalent projected area size and equivalent volume size for 38 size bins.
- Optical properties: extinction efficiency, single scatter albedo, asymmetry factor, and δ-function forward-peak factor for 38 size bins and 65 wavelengths (Yang et al., 2006).

Size distributions and weight distribution

- 30 size distributions of the ice crystals by Fu (1996)

- Baum et al. (2005):

L<60 μm comprises 100% droxtals; 60<L<1000 μm comprises 50% solid columns, 35% hexagonal plates, and 15% spatial bullet rosettes; 1000<L<2000 μm comprises 45% solid columns, 45% hollow columns,and10% aggregates; L>2000 μm comprisesj 97% spatial bullet rosettes and 3% aggregates.

Zhang et al., JQSRT, 2015

Steps of creating the new parameterization

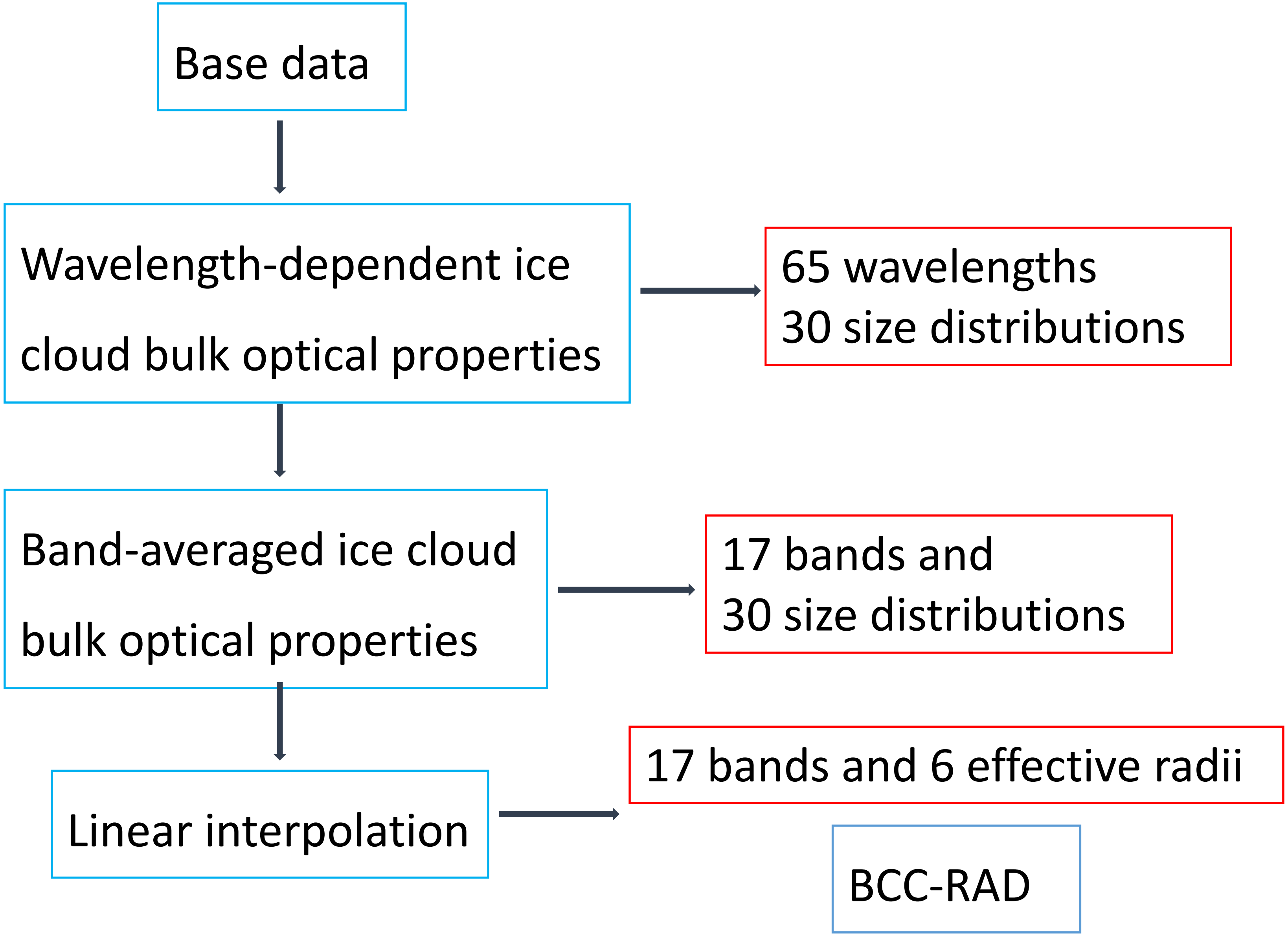

The band-averaged ice cloud bulk optical properties:

$$\overline{k_{ex}} = \frac{\int_{\lambda_{\min}}^{\lambda_{\max}} (Sun(\lambda)+\pi B(T,\lambda))k_{ex}(\lambda)d\lambda}{\int_{\lambda_{\min}}^{\lambda_{\max}} (Sun(\lambda)+\pi B(T,\lambda))d\lambda};$$

$$\overline{k_{ab}} = \frac{\int_{\lambda_{\min}}^{\lambda_{\max}} (Sun(\lambda)+\pi B(T,\lambda))k_{ab}(\lambda)d\lambda}{\int_{\lambda_{\min}}^{\lambda_{\max}} (Sun(\lambda)+\pi B(T,\lambda))d\lambda};$$

$$\bar{\omega} = 1 - \frac{\overline{k_{ab}}}{\overline{k_{ex}}};$$

$$\bar{g} = \frac{\int_{\lambda_{\min}}^{\lambda_{\max}} (Sun(\lambda)+\pi B(T,\lambda))g(\lambda)d\lambda}{\int_{\lambda_{\min}}^{\lambda_{\max}} (Sun(\lambda)+\pi B(T,\lambda))d\lambda};$$

$$\bar{f_\delta} = \frac{\int_{\lambda_{\min}}^{\lambda_{\max}} (Sun(\lambda)+\pi B(T,\lambda))f_\delta(\lambda)d\lambda}{\int_{\lambda_{\min}}^{\lambda_{\max}} (Sun(\lambda)+\pi B(T,\lambda))d\lambda};$$

$$\bar{f} = \bar{f_\delta} + \frac{1}{2\bar{\omega}}。$$

Ice Cloud Optics: Bulk Optical Properties

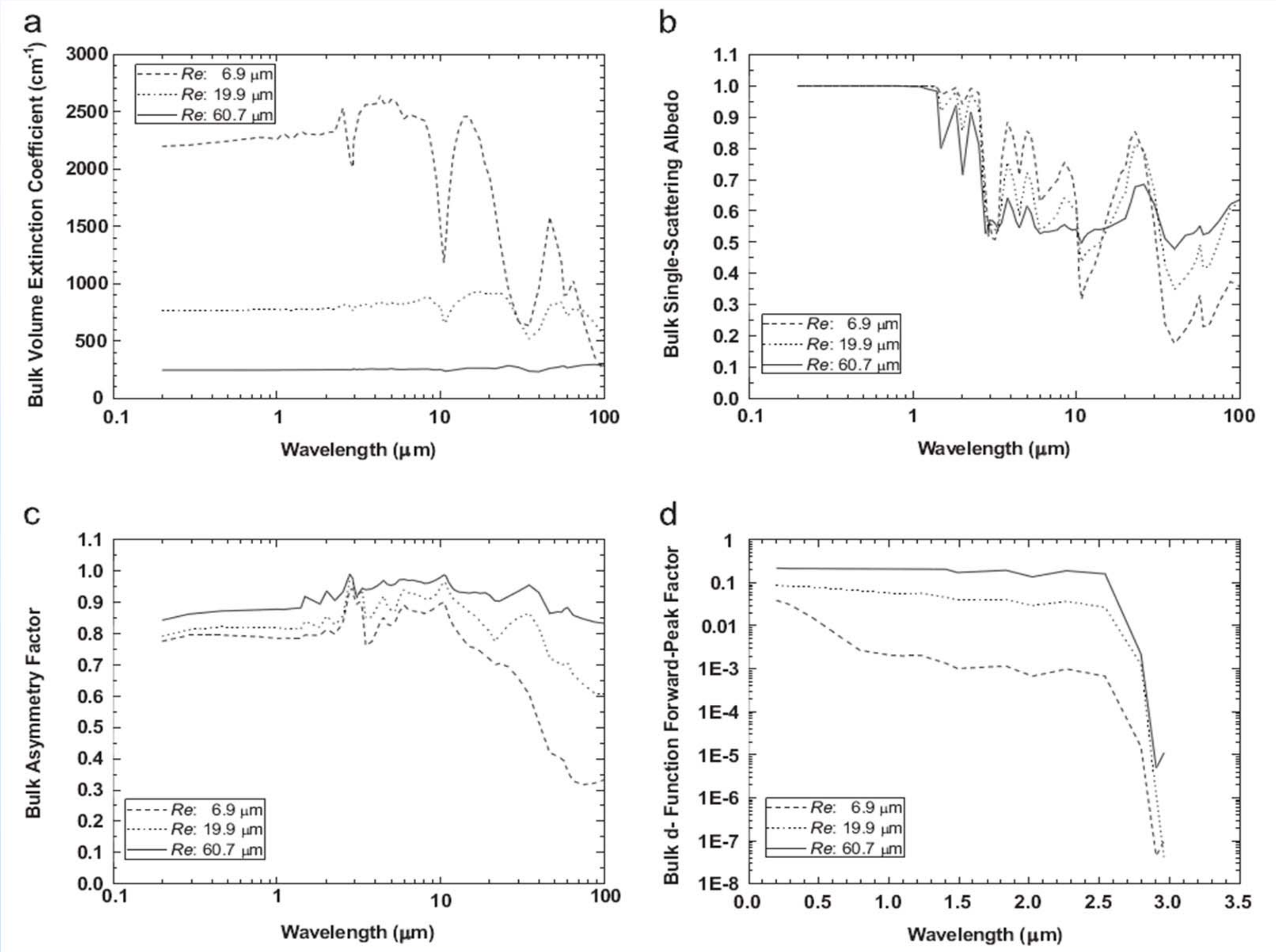

Variations in the bulk (a) extinction coefficient, (b)single scattering albedo, (c)asymmetry factor, and (d)forward-peak factor with wavelength for three size distributions.

Ice Cloud Optics: Band-averaged

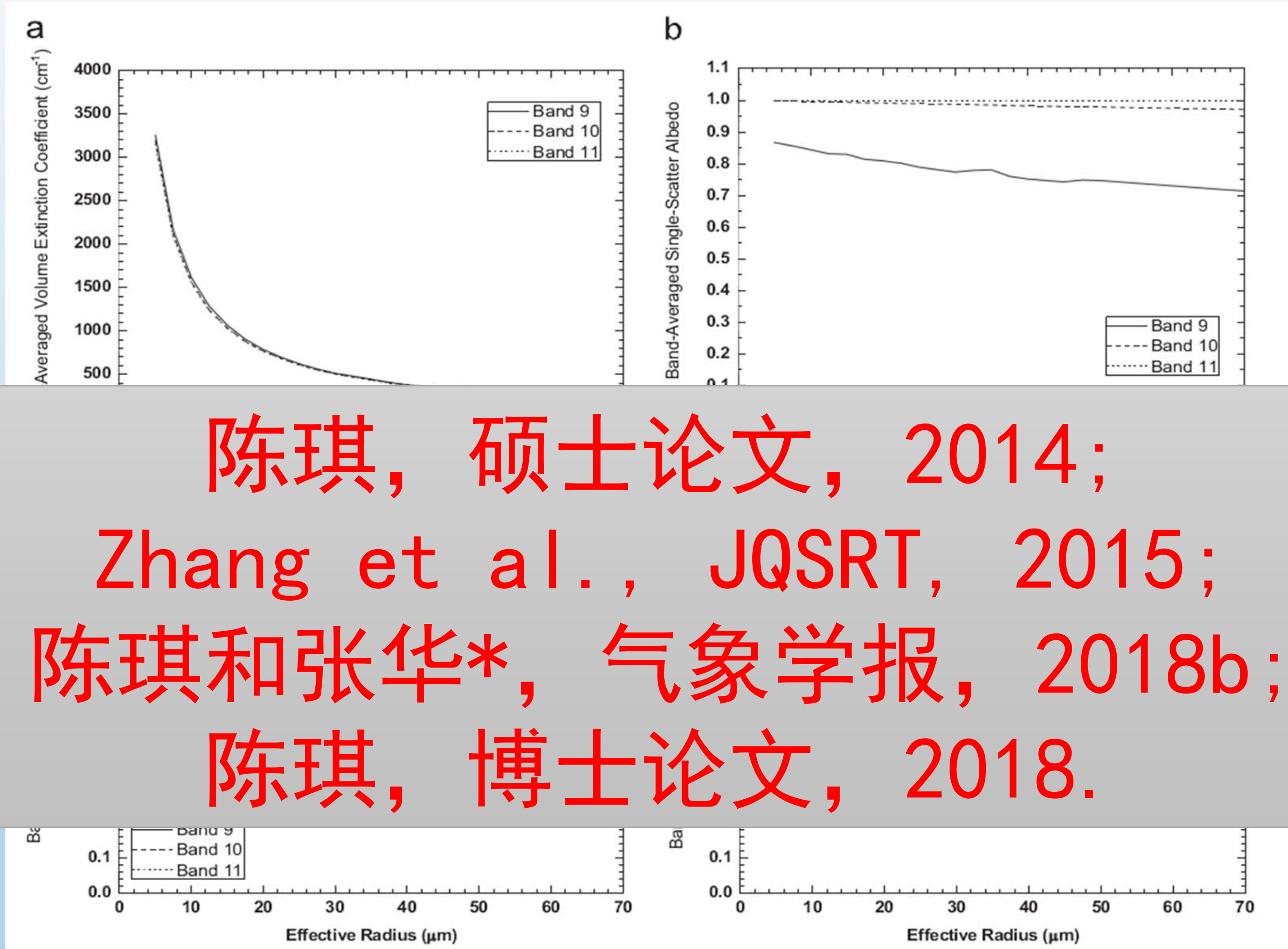

陈琪，硕士论文，2014；
Zhang et al., JQSRT, 2015;
陈琪和张华*，气象学报，2018b;
陈琪，博士论文，2018.

Variations in the band-averaged (a)extinction coefficient, (b)single-scattering albedo, (c)asymmetry factor and (d)forward-peak factor with the effective radius for three shortwave bands.

Outline

1. Correlated k-Distribution Method
2. Aerosol Optics
3. Cloud Optics
4. Radiative Transfer Algorithms
5. Comparison of BCC_RAD with other Models

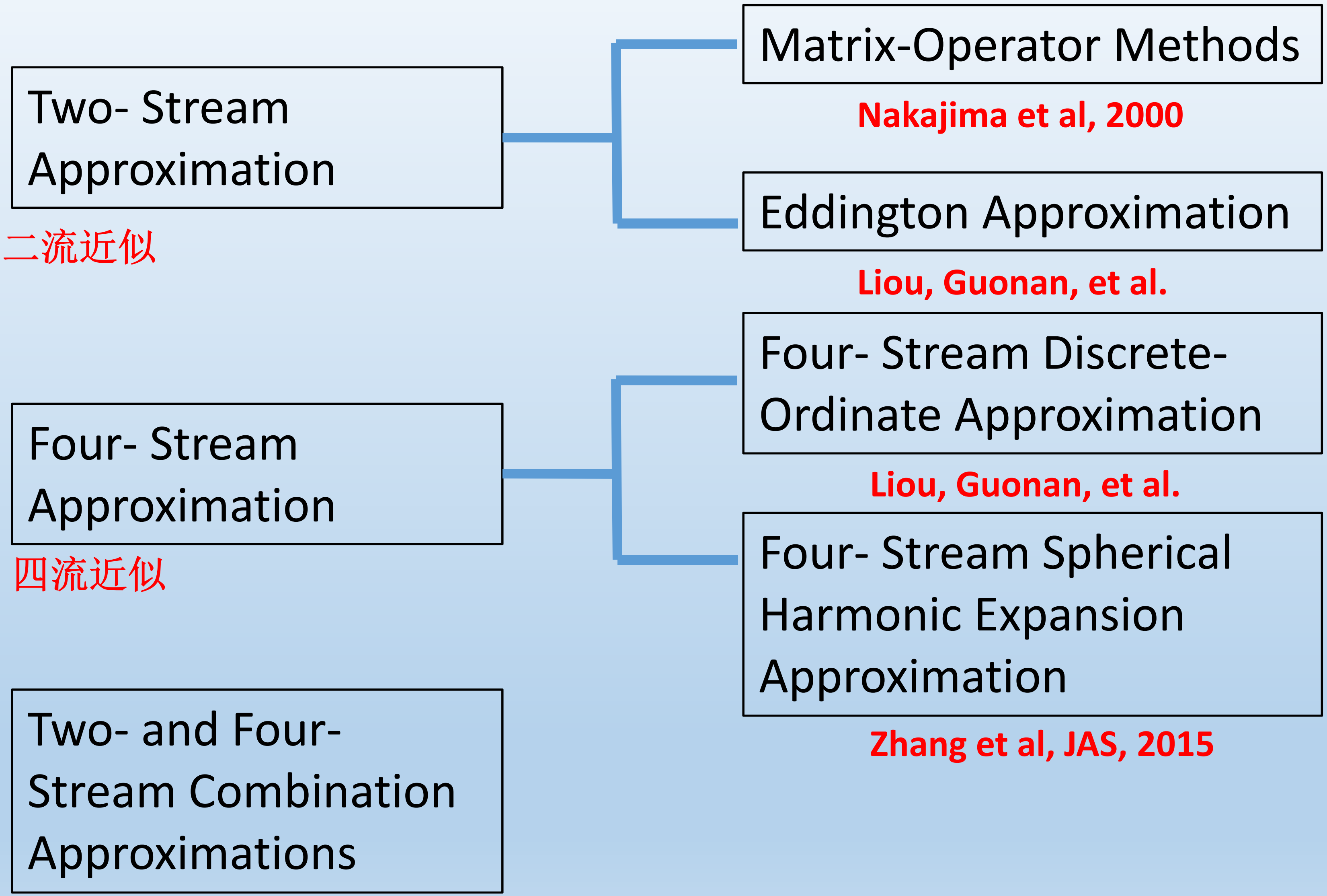

二流四流混合算法：张华和卢鹏，气象学报，2014

Outline

1. Correlated k-Distribution Method
2. Aerosol Optics
3. Cloud Optics
4. Radiative Transfer Algorithms
5. Comparison of BCC_RAD with other Models

BCC_RAD Participating CIRC
(Randles et al., ACP, 2013)

CIRC (Continual Intercomparison of Radiation Code).

Four cases in clear sky.
Solid line: LBLRTM; dotted line: BCC_RAD.

The ordinate is pressure.
The abscissas is longwave up and down flux, and cooling rate, respectively.

Results of BCC_RAD Participating in CIRC

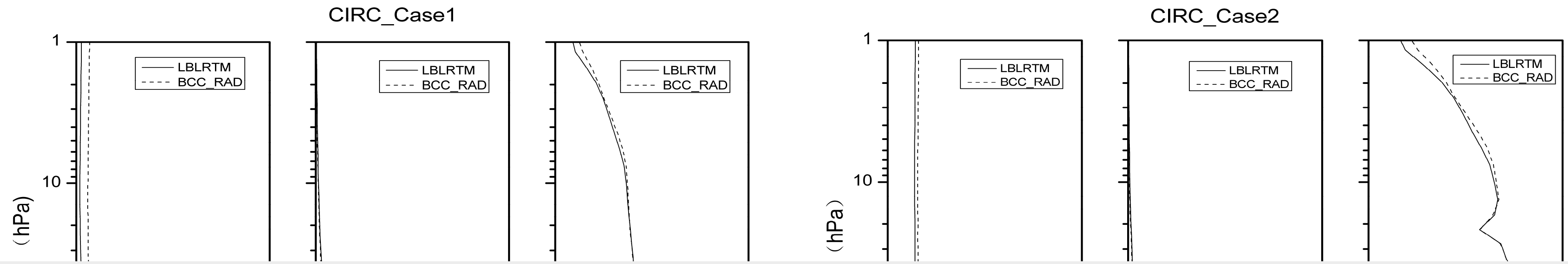

- **Comparing with LBLRTM, the results of longwave up flux of BCC_RAD are larger, but the down flux are slightly smaller.**

- **The results of cooling rate of BCC_RAD are smaller than those of LBLRTM between 40 mb and 1 mb.**

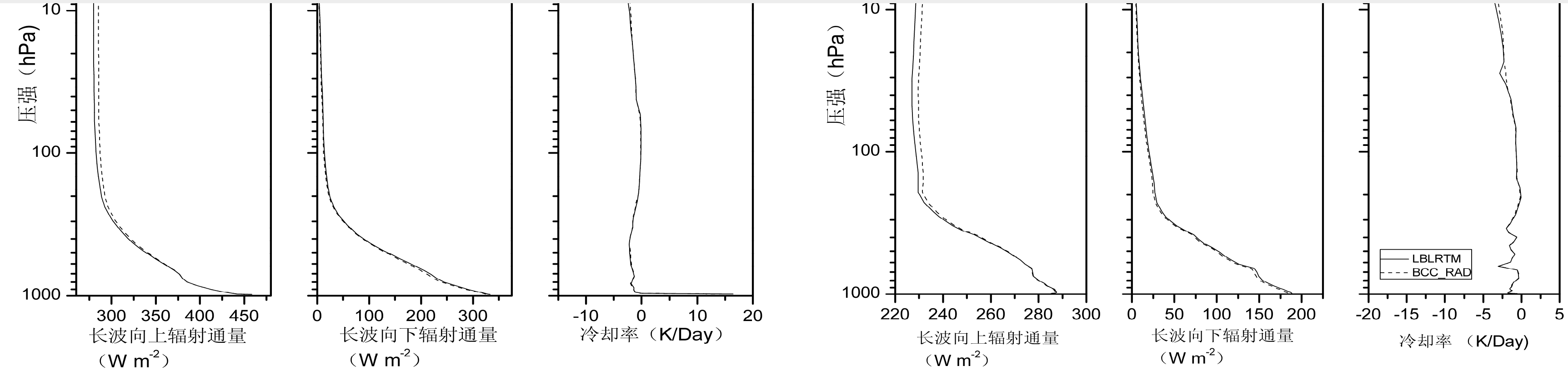

Results of BCC_RAD Participating in AeroCom

Myhre et al., ACP, 2013

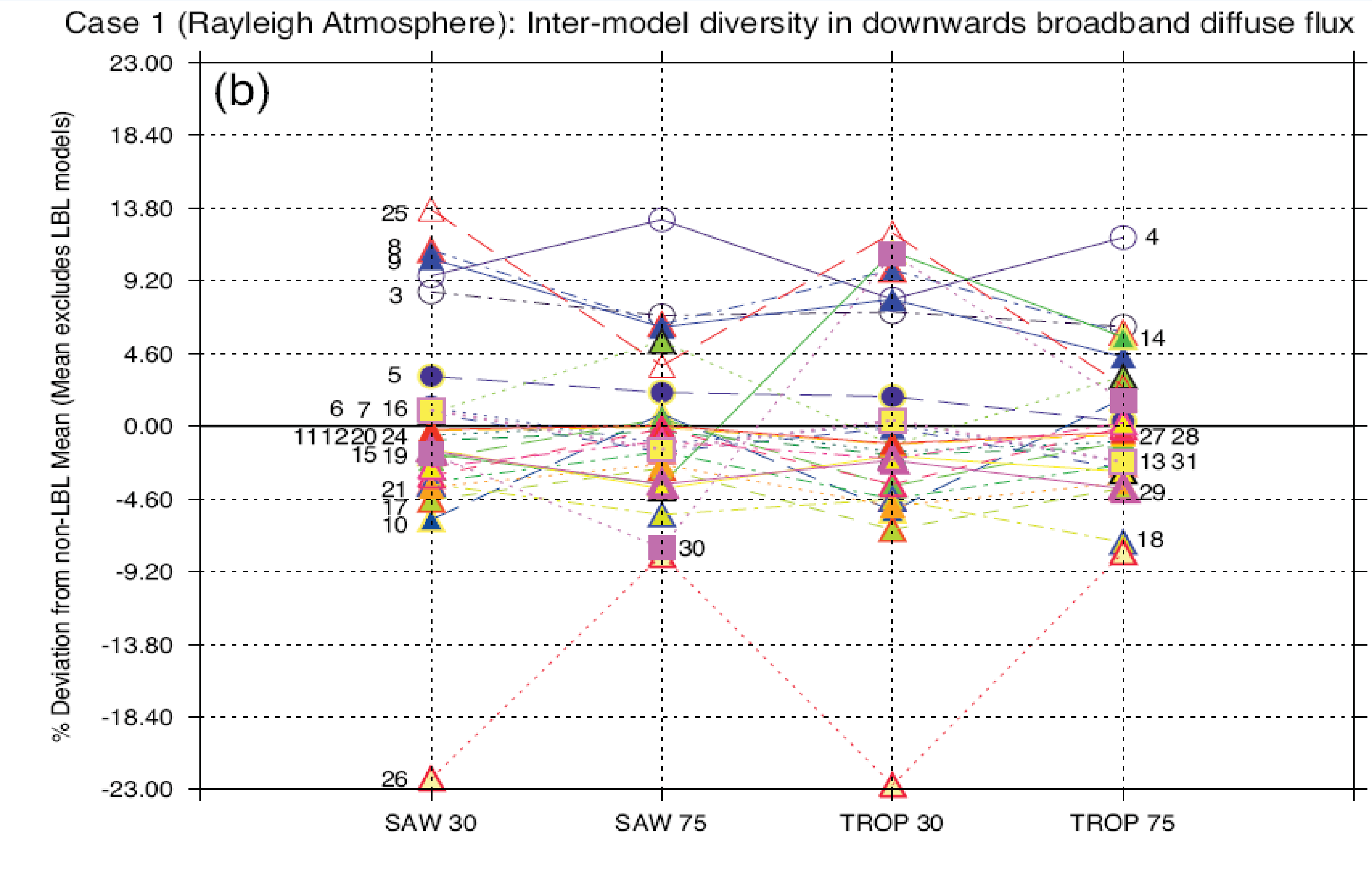

The number of BCC_RAD is 16.

The results of BCC_RAD are above the average.

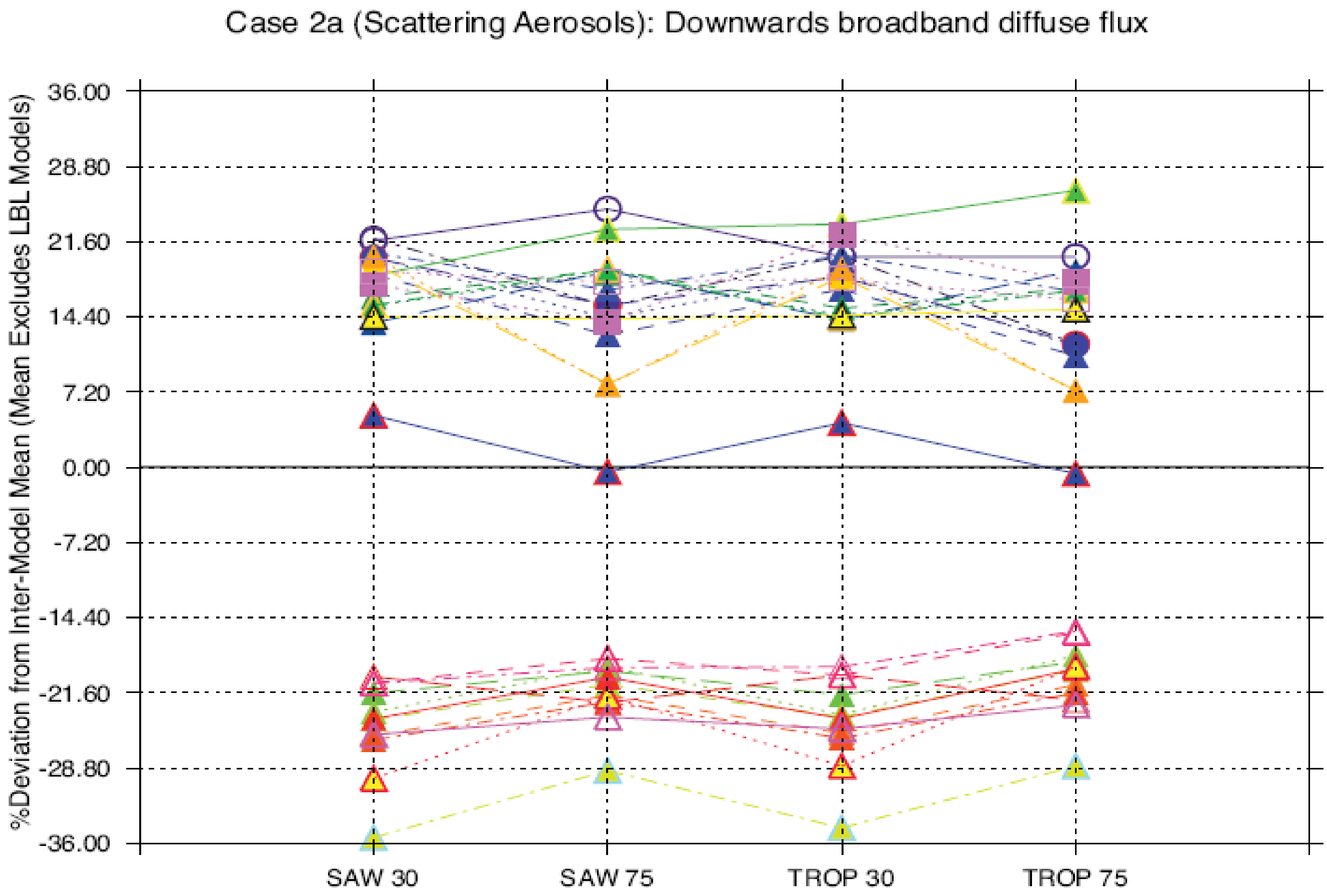
Case 2a (Scattering Aerosols): Downwards broadband diffuse flux
%Deviation from Inter-Model Mean (Mean Excludes LBL Models)
36.00
28.80
21.60
14.40
7.20
0.00
-7.20
-14.40
-21.60
-28.80
-36.00
SAW 30
SAW 75
TROP 30
TROP 75

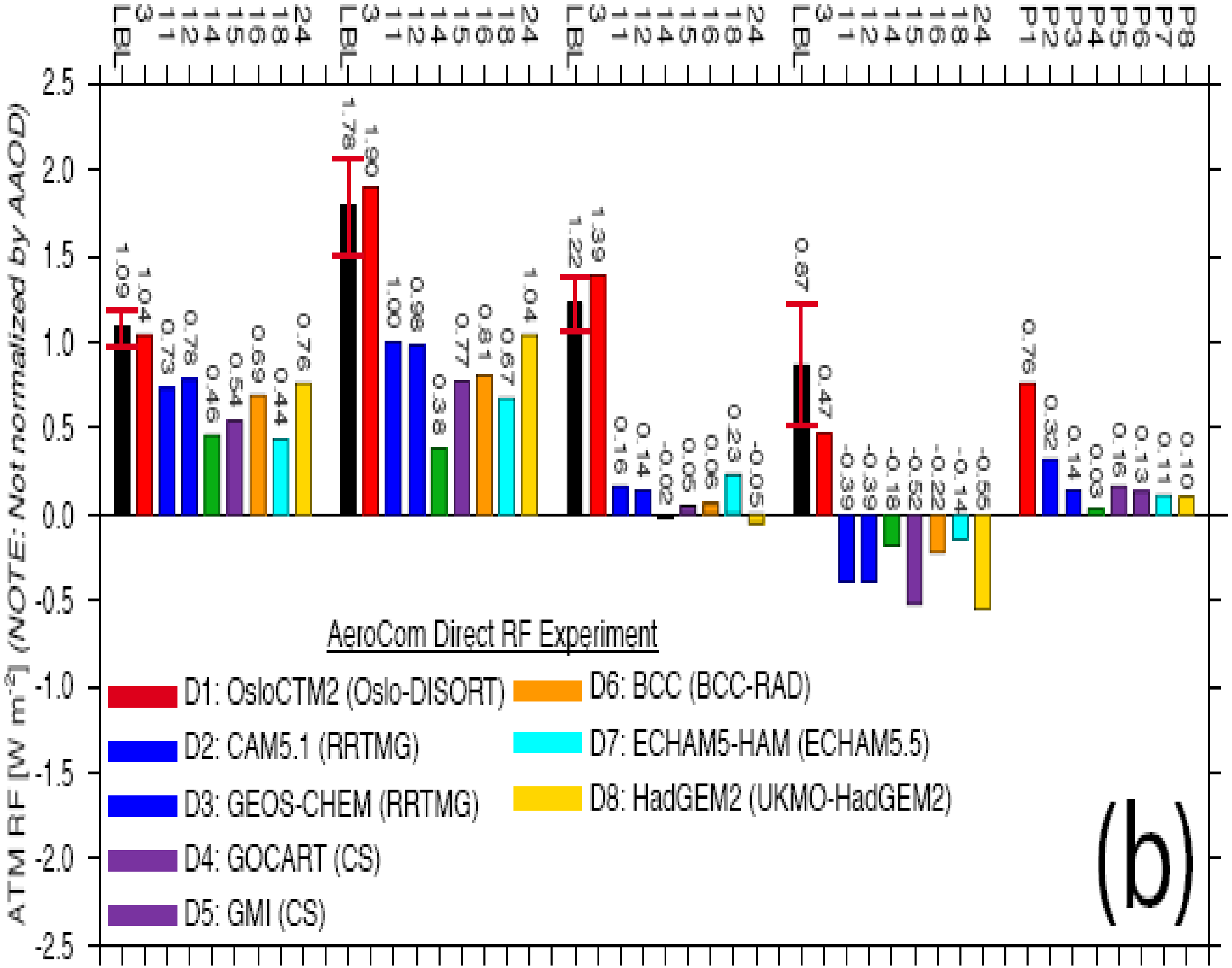
AeroCom Direct RF Experiment
D1: OsloCTM2 (Oslo-DISORT)
D2: CAM5.1 (RRTMG)
D3: GEOS-CHEM (RRTMG)
D4: GOCART (CS)
D5: GMI (CS)
D6: BCC (BCC-RAD)
D7: ECHAM5-HAM (ECHAM5.5)
D8: HadGEM2 (UKMO-HadGEM2)
(b)
ATM RF [W m^{-2}] (NOTE: Not normalized by AAOD)
LBL
3
11
12
14
15
16
18
24
P1
P2
P3
P4
P5
P6
P7
P8

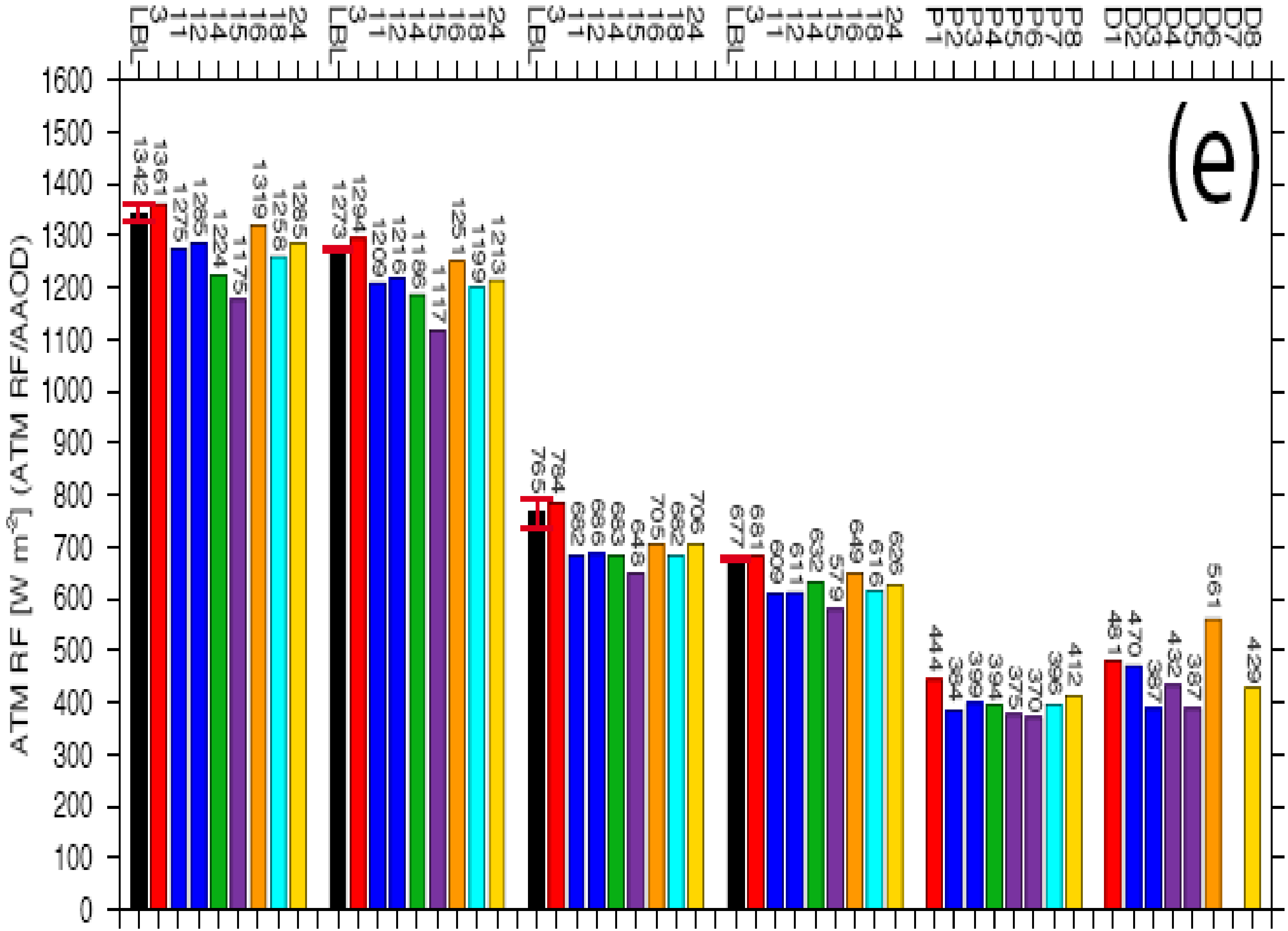
(e)
ATM RF [W m-2] (ATM RF/AAOD)
LBL
3
11
12
14
15
16
18
24
P1
P2
P3
P4
P5
P6
P7
P8
D1
D2
D3
D4
D5
D6
D7
D8
1342
1361
1275
1285
1224
1175
1319
1258
1285
1273
1294
1209
1216
1186
1117
1251
1199
1213
765
784
682
686
683
648
705
682
706
677
681
609
611
632
579
649
616
626
444
384
399
394
375
370
396
412
461
470
387
432
387
561
429


张华 编著
BCC_RAD DAQI FUSHE CHUANSHU MOS
BCC_RAD大气辐射
传输模式
气象出版社
China Meteorological Press


大气气溶胶
及其气候效应
张 华 王志立 赵树云 等◎编著
气象出版社
China Meteorological Press

Future issues:

- Updated HITRAN dataset for line and continuum;
- Optimal treatment of overlapping bands need to be further studied; more reasonable band dividing scheme and better k-interval choosing method?
- Accurate treatment for ice cloud optical properties, ice habits and their weight in ice cloud, ice particle size distribution, etc.;
- Accurate calculation for aerosol optical properties, getting observational size distribution;
- How use machine learning and large mount of dataset for radiation scheme in climate model for prediction to reduce costs for calculation in LW and SW, is it possible to replace physical scheme with machine learning scheme? The technique to choose dataset for training.
- Spectral albedo observational dataset for RT calculation.
- Cloud overlapping treatment in radiative transfer algorithm.

Thank you for your attention!